Remote Sensing of Environment 209 (2018) 291–311

Contents lists available at ScienceDirect

Remote Sensing of Environment

journal homepage: www.elsevier.com/locate/rse

Parametrizing tidal creek morphology in mature saltmarshes using semi-automated extraction from lidar

Chirol C.[a,*], Haigh I.D.[a], Pontee N.[b], Thompson C.E.[a], Gallop S.L.[c]

[a] Ocean and Earth Sciences Department, National Oceanography Centre Southampton, SO14 3ZH, UK
[b] Coastal Planning and Engineering Practice, CH2MHill, Swindon SN40QD, UK
[c] Department of Environmental Sciences, Macquarie University, NSW 2109, Australia

ARTICLE INFO

Keywords:
British isles
Channel delineation
Coastal wetlands
Creek network
Lidar
Managed realignment
Morphological equilibrium
Morphometry

ABSTRACT

Coastal saltmarshes provide a range of ecosystem services, such as flood protection and carbon sequestration, but face rapid global losses. Managed realignment (MR) is an increasingly popular method to artificially recreate these habitats by reinstating tidal regimes to reclaimed land. However, to improve MR design, better knowledge of the processes that control morphological evolution in natural saltmarshes is needed. In this paper, we develop tools to assist in the monitoring of creek network evolution towards dynamic morphological equilibrium, a state of landform stability under current physical forcings. Using lidar (Light Detection and Ranging) datasets, we combined a semi-automated creek extraction algorithm, based on elevation and slope thresholds, with a novel algorithm for morphometric creek analysis. A comprehensive suite of morphological creek characteristics was extracted for 13 natural British saltmarshes, including: amplitude, length, sinuosity ratio, junction angle, width, depth, cross-sectional area, creek order, bifurcation ratio, drainage density, and drainage efficiency. Results closely matched with field-validated manual digitization results, and were significantly faster and less subjective to produce. Morphological equilibrium relationships from the literature were found to be applicable to the new dataset, despite yielding high prediction errors due to the inherent variety of creek network shapes in saltmarshes. New equilibrium relationships were also defined relating the creek network drainage efficiency to the mouth cross-sectional area and the marsh elevation. To improve future scheme designs, these tools will be used in further studies to monitor rates of evolution towards equilibrium in MR sites depending on their initial conditions.

1. Introduction

Coastal wetlands such as saltmarshes are valuable habitats that provide a wide range of ecosystem services (Luisetti et al., 2014). They play important roles as biodiversity hotspots (Zedler and Kercher, 2005; Mossman et al., 2012), carbon sinks (Erwin, 2009; Ahn and Jones, 2013; Tempest et al., 2014), natural defences against coastal erosion and flooding (Möller and Spencer, 2002; Van Der Wal et al., 2002; Gedan et al., 2011), nurseries for juvenile fish (Luisetti et al., 2014), pollutant filters (Mudd, 2011), and sites for recreational activities (Luisetti et al., 2014). However, they have been the subject of extensive reclamation for centuries, largely for agriculture (Doody, 2004). Though accurate appraisals of losses are difficult to quantify due to the lack of quality data (Duarte et al., 2008; Foster et al., 2013), global coastal wetland decline is estimated at 25–50% over the last 150–300 years (Lotze et al., 2006), with a current global rate of saltmarsh loss estimated at 1–2% per year (Duarte et al., 2008). Despite increased awareness of their importance, the rate of loss has increased by a factor of 4.2 in recent years, largely due to sea level rise and urban development (Spencer and Harvey, 2012; Davidson, 2014).

To compensate for coastal wetland loss, the creation of new intertidal habitat through landward realignment of flood defences, also called managed realignment (MR), has been attempted in many countries such as the US (Williams et al., 2001), the UK, the Netherlands, Germany (Rupp-Armstrong and Nicholls, 2007; Chang et al., 2016) and Australia (Rogers et al., 2014). In north-western Europe, MR started around 1981, and since then 102 projects have been undertaken (Esteves, 2014). The implementation rate of MR in the UK still needs to increase fivefold to comply with Shoreline Management Plans that aim to realign 550 km of coastline by 2030 (Committee on Climate Change, 2017).

Morphological equilibrium implies a degree of stability in a

* Corresponding author.
E-mail addresses: cc4v12@soton.ac.uk (C. Chirol), I.D.Haigh@soton.ac.uk (I.D. Haigh), Nigel.Pontee@ch2m.com (N. Pontee), celt1@noc.soton.ac.uk (C.E. Thompson), shari.gallop@mq.edu.au (S.L. Gallop).

https://doi.org/10.1016/j.rse.2017.11.012
Received 30 March 2017; Received in revised form 31 October 2017; Accepted 10 November 2017
Available online 19 March 2018

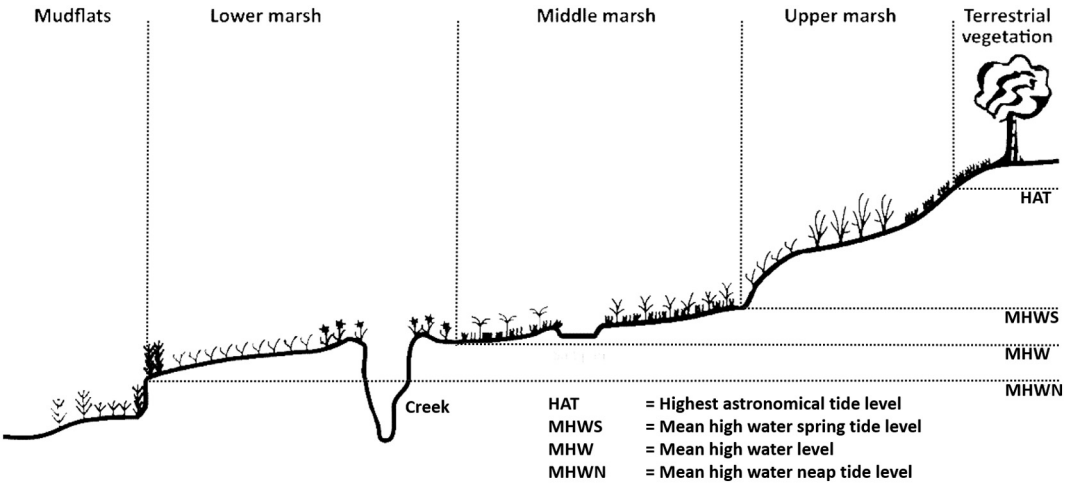

Fig. 1. Mature mudflat and saltmarsh zonation within the tidal frame. Modified from Foster et al., 2013.

landform under stable input conditions. Relatively small changes in input conditions lead to corresponding changes in the landform over timescales of decades to centuries, which is typically referred to as dynamic equilibrium (Friedrichs and Perry, 2001). In the case of saltmarshes, the key landform characteristics are the surface elevation, standing between mean high water levels and the highest astronomical tide (HAT) (Steel, 1996, Fig. 1), and the dimensions and planform of the creek network (French and Stoddart, 2001; Allen, 2000). To be considered successful, MR schemes should emulate natural systems and evolve towards a state of dynamic morphological equilibrium within similar timescales (Friedrichs et al. 2001). However, better knowledge of the physical processes controlling this evolution is needed to improve MR design (J.B.l et al., 1997; Williams et al., 2001; Pontee, 2015). A study of 18 MR schemes in the UK found that they systematically failed to replicate the plant community composition of nearby natural marshes (Mossman et al., 2012), suggesting that current schemes fail to satisfactorily reproduce physical processes.

Among other morphological features, such as the breach area and elevation distribution of the site (Townend, 2008), the creek network is an integral component of MR scheme design and success (Reed et al., 1999; Williams et al., 2002). Creek networks are important for saltmarsh ecosystem structure and function: they distribute water and nutrients, drain the site during the ebb tide, control the distribution of vegetation (Sanderson et al., 2001; Zheng et al., 2016), influence accretion rates (Reed et al., 1999), and provide habitat for juvenile fish (Miller and Simenstad, 1997).

Excavating initial channels may speed up the development of the creek network (Wallace et al., 2005). Consequently, some MR design strategies have opted to dig artificial creeks. This was first attempted in San Francisco Bay in 1980 (Williams et al., 2001), and more systematically in recent UK schemes (Tovey et al., 2009). Because of the lack of creek design guidelines, various initial shapes have been tested in the UK over the past 20 years. These design choices range from single linear distribution channels, as in Alkborough (Manson and Pinnington, 2012) and Freiston (Symonds, 2006), to more complex configurations mimicking mature network morphologies, like at Hesketh Out Marsh West (Tovey et al., 2009). However, more monitoring of creek network evolution in MR schemes is needed to assess the relative efficiency of the various strategies adopted. Previous studies on creek networks in natural saltmarshes have resulted in the definition of morphological equilibrium relationships (Steel, 1996; Williams et al., 2002; Marani et al., 2003), but their predictive values for MR design have not been investigated.

Due to lack of field surveying, the monitoring of natural and artificial creek networks relies heavily on remote sensing data, such as aerial photography or elevation maps from lidar (Light Detection and Ranging). The use of lidar is increasing due to its accessibility in many countries, extensive coverage (*e.g.*, all of the UK territory), high horizontal resolution (up to 0.25 m horizontally), and the possibility to compare datasets over consecutive years to infer evolution rates. Even though vertical uncertainty of lidar in waterlogged, low vegetation areas like coastal wetlands may complicate elevation change monitoring (Wang et al., 2009a), it is well suited to monitoring the planform evolution of large structures like creek networks.

The aim of this paper is to develop tools that will assist in the monitoring of creek network evolution towards morphological equilibrium using lidar data. To that end, we pursued three objectives:

(1) Test the efficiency of a newly developed semi-automated creek parametrization algorithm for extracting creek morphology in both natural and artificial saltmarshes;
(2) Assess the applicability and predictive value of existing creek network morphological equilibrium relationships using parameters extracted from our algorithm; and
(3) Establish new equilibrium relationships linking the drainage efficiency of the creek network to initial morphological conditions and tidal forcing, to be used as a MR design tool.

Before fulfilling these objectives, this paper reviews the state of knowledge in creek network development to provide a more detailed qualitative definition of the equilibrium state for a saltmarsh and a creek network. The paper then describes creek network monitoring techniques and highlights knowledge gaps addressed by our algorithm.

2. State of knowledge in creek network development

2.1. Conceptual model of creek network evolution

In this section, we briefly review processes driving creek network evolution towards morphological equilibrium in a saltmarsh. Creek networks consist of an intricate system of bifurcating channels (Coco et al., 2013) in shallow coastal environments that drive the exchange of sediment and water between estuaries and wetlands. Their stability depends on a delicate balance between sedimentary processes and hydrodynamics (Coco et al., 2013). Creek networks were first thought to develop in a similar way to fluvial channels by the erosive action of a unidirectional flow, with the draining of the ebb tide as the main driver (Lohani et al., 2006). However, tidal and wave energy dissipated on the flood tide also plays a significant role (Lohani et al., 2006): caution should be applied when comparing tidal creeks to fluvial systems. In

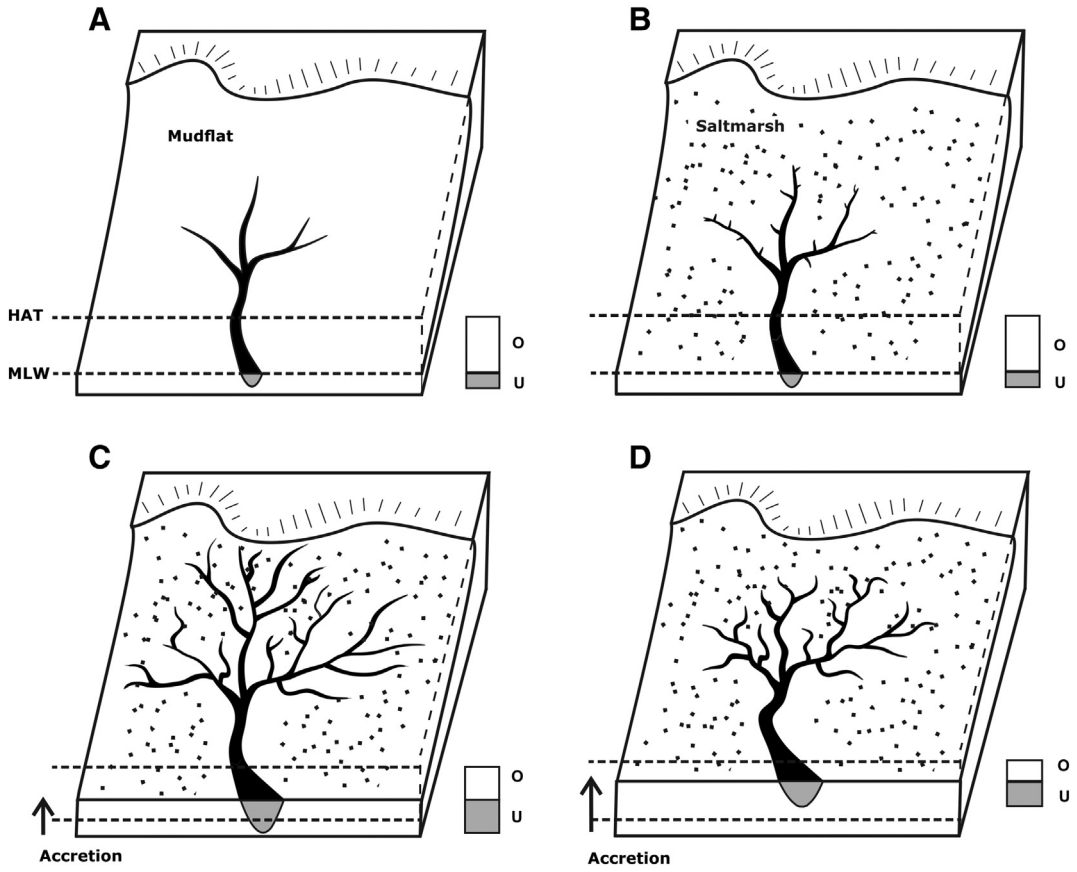

Fig. 2. Conceptual model showing the initiation (A) and development of a tidal creek network towards a state of dynamic equilibrium with the tidal forcings as the wetland accretes vertically and transitions from mudflat to saltmarsh (B–D). Modified from Steel and Pye, 1997. HAT: highest astronomical tide. MLW: mean low water. O: overmarsh tidal prism. U: undermarsh tidal prism.

order to describe what proportion of the tide is distributed through the creek network rather than through over-ground flow over the marsh surface, a distinction is made between the undermarsh tidal prism, the volume of water that the creek network can contain, and the overmarsh tidal prism, the volume of water the saltmarsh can contain between the marsh level and the Highest Astronomical Tide level (HAT) (Vandenbruwaene et al., 2012).

According to Steel and Pye's (1997) evolution model, the development of a creek network occurs in four main stages (Fig. 2). Stage A sees the tide-controlled initiation of the creek network on the unvegetated tidal flat. Most of the water exchange occurs through the overmarsh tidal prism (marked O in Fig. 2). In stage B, vegetation colonization triggers a transition from mudflat to saltmarsh and fixes the creek network (Temmerman et al., 2005; Vandenbruwaene et al., 2013). In stage C, the marsh accretes vertically in response to the low energy hydrodynamic conditions and the trapping action of the vegetation, encouraging the deposition of organic and inorganic sediment (D'Alpaos et al., 2007; Vandenbruwaene et al., 2013). The elevation gradient enhances water energy in the channels, causing their deepening and the appearance of new, smaller creeks by headward erosion (D'Alpaos et al., 2005). This produces a positive feedback loop: the increasing creek volume leads to a larger undermarsh tidal prism (marked U in Fig. 2), while the overmarsh tidal prism diminishes as a result of vertical accretion, so most of the tidal energy is forced through the creek system. In stage D, however, the elevation is such that only the larger tidal events affect the upper marsh. The drainage density decreases and the creeks farthest from the estuary are abandoned. The creek network is then considered to be at dynamic equilibrium with the tidal range: in case of rising sea level, the saltmarsh can be expected to return to stage C (Steel and Pye, 1997).

The development of creek networks towards equilibrium can take 4 to 13 years (Williams et al., 2002), though the evolution rate and the equilibrium morphology vary depending on local conditions such as antecedent geology, sediment type, vegetation cover, tidal and wave regime, and frequency of drainage pattern 'resetting' by storm events (Hughes, 2012). Finally the presence of relic features, such as agricultural drainage trenches, can influence the development of a creek network by constraining it to a particular morphology (Crooks et al., 2002). The latter factor is expected to concern most MR schemes as they dominantly occur in reclaimed agricultural lands. Also, the starting elevation of MR sites will likely differ from that of a natural stage A mudflat (Fig. 2): it may be lower due to a lack of post-reclamation sedimentation, or conversely higher in the case of a recently reclaimed saltmarsh. The presence of a breached seawall in most MR sites may also change the flow regime within the saltmarsh by constraining the flow to the creek system (Hood, 2014).

For all of these reasons, the development of creek networks in MR schemes is likely to differ from that of a natural system, and a separate conceptual model of their evolution may be needed. Thorough monitoring of creek network evolution, using a reliable creek extraction tool, must be conducted to establish these differences.

2.2. Creek network detection and parametrization

One key challenge of saltmarsh morphological studies is mapping complex features over large areas. Elevation maps from lidar successfully address this issue due to their wide availability. However, creek networks are still mainly extracted through manual digitization, then corrected with field surveys. That method is too time-consuming, expensive and subjective for large-scale monitoring projects (Mason and

Scott, 2004).

Methods for automating the creek extraction process have been explored in various studies. A common method is the eight direction (D8) flow accumulation model (Ozdemir and Bird, 2009; Passalacqua et al., 2010; Lang et al., 2012). This hydrodynamic detection tool produces a one-pixel wide flow path, corresponding to the channel centreline, but does not detect the creek planform area. In addition, tidal channel development does not depend solely on the runoff measured by flow accumulation, but also on other topographic and erodibility factors, making the D8 method at best a first approximation of a creek network (James and Hunt, 2010). This is especially true for artificial creeks, which are primarily shaped by human intervention rather than in response to hydrodynamic forces. Therefore, the creek network should be defined by its artificially chosen morphological template rather than by the flow conditions.

Alternative semi-automated creek extraction methods using lidar rely on elevation and slope or curvature thresholds (threshold methods), determined with sensitivity tests (Fagherazzi et al., 1999; Lohani et al., 2006; Mason et al., 2006; Lashermes et al., 2007; Liu et al., 2015). Due to the complexity of tidal channels, no entirely automated method has been developed, and manual corrections are often necessary. A recent method (Liu et al., 2015) comes close to full automation by enhancing and extracting Gaussian-shaped cross-sections from lidar data, corresponding to channels. Though the method seems promising for natural saltmarshes, initial testing showed that it may not apply to artificially excavated creek networks in MR sites as they can assume a variety of shapes other than Gaussian (*i.e.* rectangle, terraces or multimodal curve). Therefore, we opted for the threshold method as it is more intuitive and is based on a less restrictive definition of a creek network, while being faster and less subjective than manual extraction.

Although some previous studies have manually extracted creek cross-sections to infer volumetric parameters (Mason et al., 2006), none of the currently proposed algorithms include a fully automated parameter extraction routine. This makes them poorly adapted to morphological interpretation, and does not exploit the full potential of lidar data. The added value of our new technique compared to traditional algorithms is that it extracts a comprehensive list of parameters, such as length, width, depth, cross-sectional area, sinuosity, junction angle, bifurcation ratio, and drainage efficiency, for all creeks, with minimal user inputs. The creek extraction algorithm presented herein is one of the first to provide results directly interpretable by geomorphologists. The paper tests this algorithm on lidar data collected at 13 natural saltmarshes.

3. Study sites and data

The thirteen UK saltmarshes used for this study cover a wide range of environmental settings. The sites are located in Moricambe Bay (Solway Firth), the Ribble Estuary, the Dyfi Estuary, the Loughor Estuary, the Severn Estuary, the Beaulieu Estuary, the Swale Estuary, Dengie Peninsula, Tollesbury Fleet, the north Norfolk coast, and the Wash (Fig. 3).

The sites were first selected by Steel (1996), who used several criteria to ensure they were representative of mature natural saltmarshes, such as being unaffected by human activity and receiving no terrestrial discharge. Steel (1996) also explored the history of the saltmarshes to verify their stability: as of 1996, they were estimated by literature analysis to be 30 years to over 2000 years old (Table 1). Marshes displaying frontal erosion were generally avoided, though some erosion was observed at Grange, Hen Hafod and Newton Arlosh. At each site, a single creek network was identified by Steel (1996) and morphological parameters extracted using aerial photograph analysis and field surveys. Information about the saltmarshes' sediment cohesive properties was given by the percentage of material of < 20 μm (Mehta and Lee, 1994) found in the literature (Steel, 1996, Table 1).

Recent nearest neighbor interpolated lidar datasets at a 1 m horizontal resolution were obtained for all 13 sites (Table 1). Contrary to other interpolation methods, nearest neighbor preserves variations in the data such as ~1 m channels which would otherwise be smoothed over (Lohani and Mason, 2001), making this method particularly adapted to representing a creek network (Rapinel et al., 2015). The data was collected by the Environment Agency (EA) and Natural Resources Wales, and accessed *via* the survey open data (https://data.gov.uk/) and Lle download portals (http://lle.gov.wales/Catalogue/Item/LidarCompositeDataset/), respectively. This freely available data comes in two forms: raw Digital Surface Model (DSM), which gives the point of first laser beam return, and Digital Terrain Model (DTM) where the above-ground features such as buildings and vegetation have been filtered out (Liu, 2008).

Quality analysis performed on consecutive EA collected lidar datasets from 2008 until 2014 showed discrepancies of about 0.3 m between the DSM and DTM, which can be assumed to be mainly due to vegetation removal. Indeed most discrepancies occurred in and around the creek network, where the near-infrared laser beam is likely to be reflected by vegetation cover, reflected from the water surface, or absorbed within the water column (Brzank et al., 2008; Wang et al., 2009a). This means bed elevation cannot be measured under the water surface, which is not usually a problem since lidar data are collected at low tide when most tidal channels are fully drained.

There was a lack of consistency in the vegetation removal algorithm results over consecutive years, possibly due to changes in the EA algorithm since 2008. As the detailed algorithm(s) were not made publically available at the time of study and could constitute a significant source of error, the DTMs were considered unreliable and the raw DSMs were chosen instead. We assumed that the low saltmarsh vegetation is unlikely to mask the creek network or significantly affect the detection of creek edges in the DSM. This choice may lead to underestimation of the channel depth, if the laser beam is reflected or absorbed by residual water within the creek during low tide. Using the DSM could also lead to overestimation of the saltmarsh elevation if the vegetation cover is detected as the ground level, and could limit the monitoring of accretion rates when analyzing MR evolution over consecutive years (Wang et al., 2009a; Hladik et al., 2013).

Tidal levels relevant to mudflat and saltmarsh zonation were extracted for all sites from the Admiralty tide data (Admiralty Tide Tables, 2014, Fig. 1). To infer the tidal range, we focused on the larger tidal events that occur when the sun, moon and Earth are aligned roughly every 14 days, called spring tides. For each site, the highest astronomical tide (HAT), mean high water spring (MHWS), and mean low water spring (MLWS) tidal levels were interpolated from the weighted mean of the surrounding main and secondary ports. We subtracted MHWL to MHWS to get the mean spring tidal ranges (MSTR). The tidal asymmetry was approximated by the ratio of the mean flood and ebb periods, each taken as the average of three representative spring and three representative neap tidal cycles.

4. Methodology

In order to fulfill the first objective of this paper, we developed a semi-automated creek parametrization algorithm using Matlab R 2015a. The main steps undertaken are summarized in Fig. 4 and explained in the sections below.

4.1. Preprocessing

Preprocessing of lidar data using ArcGIS 10.2.2 involved merging mosaics into a single dataset, georeferencing to UK National Grid, interpolating gaps to the values of the nearest neighbors according to Euclidean distance, clipping to the saltmarsh area, and extracting both elevation and slope maps. Visual observation found creek edges to be more visible on the slope than on the curvature map for our datasets, so the slope was chosen as a threshold parameter unlike previous studies

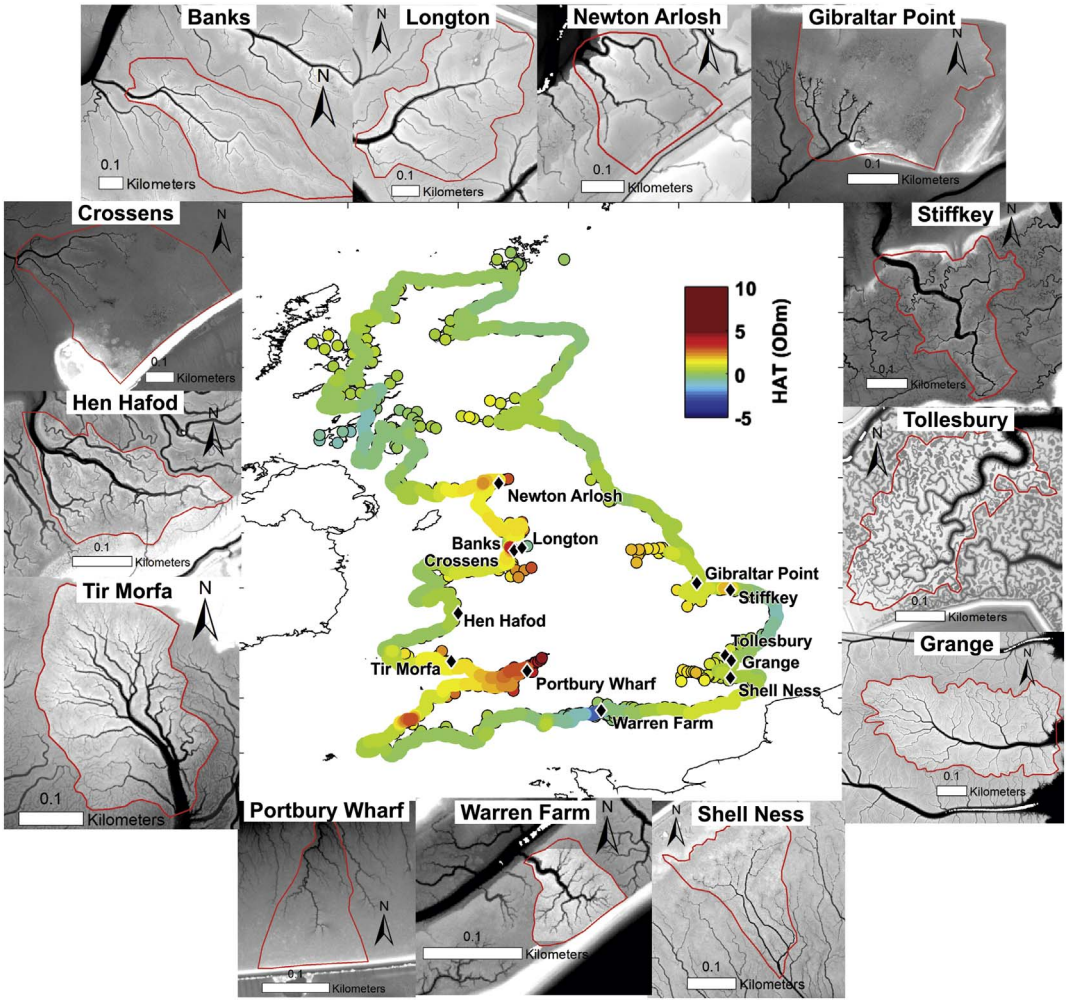

Fig. 3. Location of the 13 mature natural saltmarshes selected for this study. Colorbar shows the highest astronomical tide along the British coastline established through linear interpolation of the Admiralty Tide data (Admiralty Tide Tables, 2014). Red line shows the catchment area contours of each creek system considered. (For interpretation of the references to color in this figure legend, the reader is referred to the web version of this article.)

(Fagherazzi et al., 1999). The chosen preprocessing steps, though minimalistic, fit with our goal of providing monitoring tools reusable by MR designers for future schemes. Indeed, we test the accuracy of creek parameters detected from freely available lidar DSM that have undergone minimal preprocessing, as is likely to be the case for most of the MR monitoring work performed by the EA and consulting companies due to time constraints.

In MR schemes, clipping to the saltmarsh area is facilitated by the presence of seawalls, which constrain the influence of the tide. In the present study, however, the catchment areas were delimited following

Table 1
Location and physical characteristics of the 13 British natural saltmarshes considered in this study. The OS grid reference corresponds to the pour point of the entry channel.

Marsh name/location	O.S. grid reference	Age (estimated in 1996)	Lidar collection year	Catchment area (km^2)	Mean marsh gradient ($*10^{-3}$)	< 20 μm sediment % (Steel, 1996)
Warren Farm/Beaulieu estuary	SZ4225097275	~110	2014	0.006	1.4	46
Tollesbury/Blackwater estuary	TL9609112003	> 500	2008	0.081	0.24	65
Grange/Dengie Peninsula	TM0384802264	~110	2014	0.169	0.91	30
Hen Hafod/Dyfi Estuary	SN6488694902	~70	2015	0.040	0.54	25
Tir Morfa/Loughor Estuary	SS5308697743	~65	2010	0.069	1.30	26
Stiffkey/North Norfolk	TF9751844481	> 2000	2014	0.073	0.45	21
Banks/Ribble Estuary	SD3693822645	~120	2014	0.260	0.26	29
Crossens/Ribble Estuary	SD3502421112	~50	2014	0.243	0.98	15
Longton/Ribble Estuary	SD4465526146	> 220	2014	0.227	0.46	25
Portbury Wharf/Severn Estuary	ST4862577476	~70	2009	0.016	6.20	67
Newton Arlosh/Solway Firth	NY1936156388	> 170	2013	0.067	0.46	3
Shell Ness/The Swale Estuary	TR0461167413	~70	2014	0.045	0.34	59
Gibraltar Point/The Wash	TF5581657517	~50	2014	0.088	0.44	20

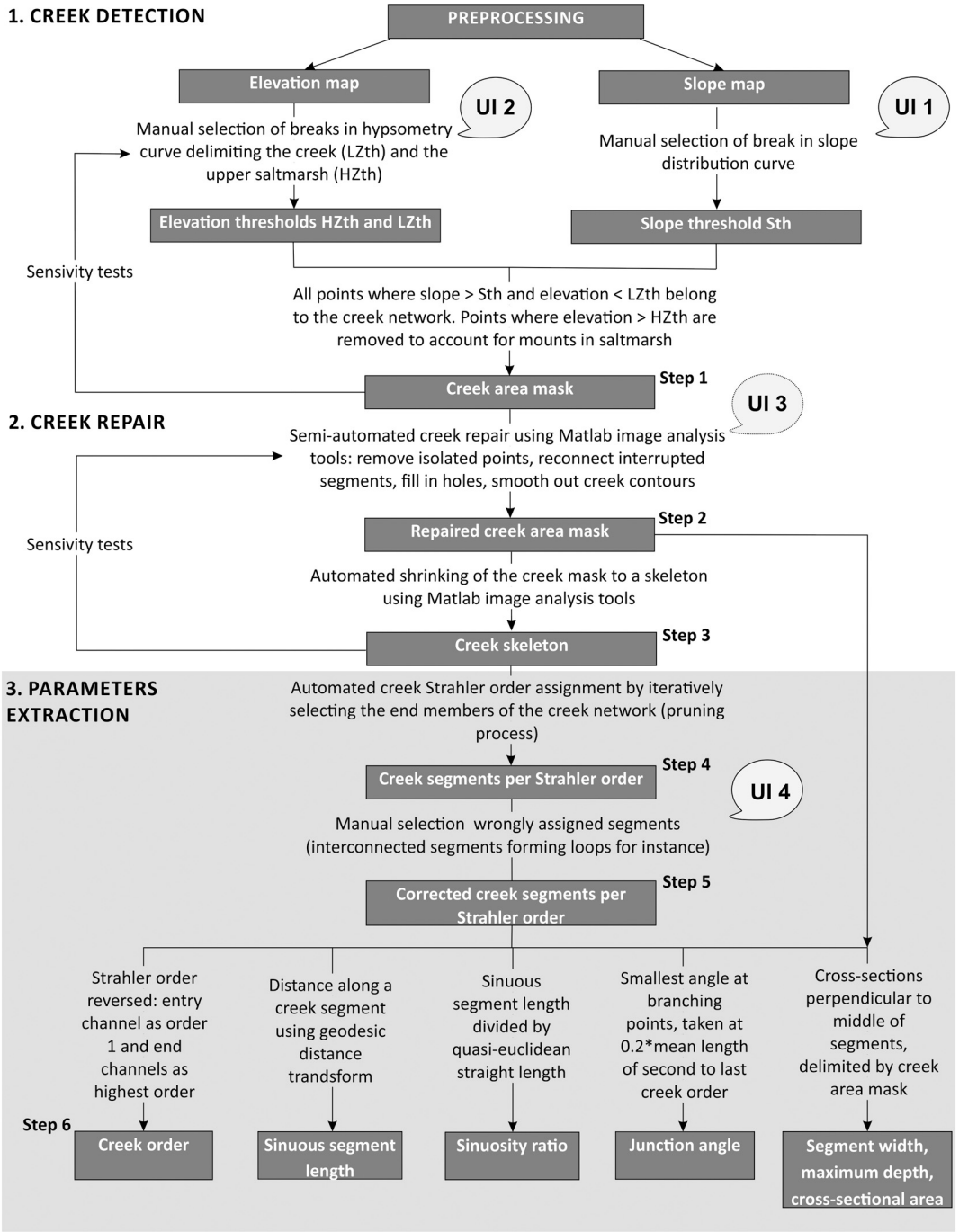

Fig. 4. The creek parametrization algorithm workflow comprises 6 processing steps and can be broken down into three phases: creek detection (step 1); creek repair (steps 2 and 3) and parameter extraction (steps 4 to 6). The steps where user inputs (UIs) are necessary are marked as UI 1 to 4.

Steel's (1996) criteria to facilitate comparison of results. The seawards limit was defined as the mouth of the entry channel, which serves as outlet for all the considered creek network. The landward limit was defined as the local HAT level, corresponding to the limit between the tidally influenced saltmarsh and the land. Finally, Steel (1996) defined the lateral limits of the saltmarsh as the halfway point between the studied creek network and the adjacent drainage system. Unlike fluvial drainage basins, saltmarsh catchment boundaries cannot be directly inferred from drainage divides in the elevation map, as drainage directions vary both in space and time due to the bidirectional tidal flow (Steel, 1996; Marani et al., 2003). Also, a hydrodynamic approach based on the estimation of water surface topography found drainage divides to be equidistant between channels (Marani et al., 2003), so the half-way distance was considered a good estimation of the catchment area lateral limits for this study. The catchment areas thus delimited only differed from Steel's when the creek network had expanded between the two studies. The two outputs of this preprocessing phase, an elevation map and a slope map in degrees, both at a horizontal resolution of 1 m, were converted into text files and exported to Matlab for the processing phase.

4.2. Creek network parametrization workflow

This section details the workflow of our algorithm, which takes as input two text files containing elevation and slope maps at 1 m resolution, and comprises three main phases: 1) creek detection; 2) creek

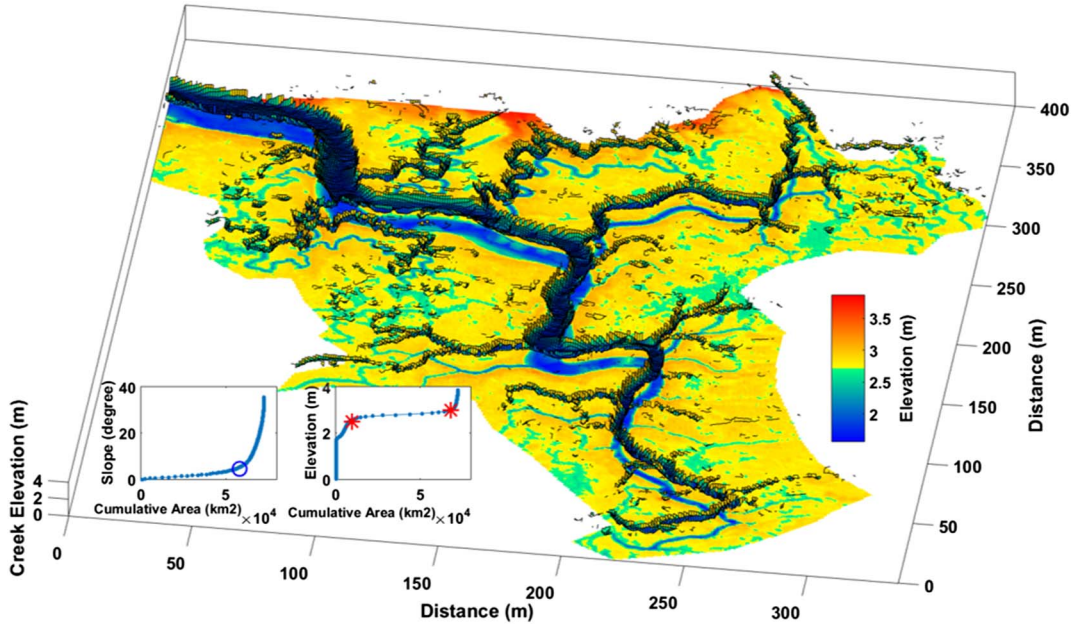

Fig. 5. Creek elevation and slope threshold detection at Stiffkey Marsh (step 1). Sth: blue circle. HZth, LZth: red asterisks. The pixels detected with those thresholds are displayed in black over the Lidar elevation map. (For interpretation of the references to color in this figure legend, the reader is referred to the web version of this article.)

path repair; and 3) morphological parameter extraction (Fig. 4).

4.2.1. Creek detection

First, a disconnected, noisy creek network mask is created using elevation and slope thresholds (Step 1, Fig. 4). All points below the elevation threshold LZth correspond to the bottom of channels, and all points above the slope threshold Sth correspond to channel edges. In order to avoid detecting mounts or the edges of a flood defence, all points higher than the upper marsh elevation threshold HZth are removed from the results. LZth, HZth and Sth are selected near the breaking points of slope and elevation distribution curves (User Input (UI) 1 and 2, Fig. 4), then refined by trial and error adjustments to obtain a creek layout similar to that visually observable in the lidar map (Fig. 5).

4.2.2. Creek repair

After the initial creek detection phase, the noise from the raw creek masks (Fig. 6A) is filtered using the image analysis function *bwareaopen* in Matlab (UI 3, Fig. 4). Fragmented terminal channels are then reconnected to the creek system (Step 2, Fig. 4): the unconnected objects are selected in ascending order, and the shortest Euclidean distance to the rest of the network is chosen as the repair path (Fig. 6B). This method can be a source of error as the repair path is only 1 pixel wide so channel width can be underestimated within the reconnected segments (Fig. 6C). This error was considered negligible due to the small contribution of terminal channels to the creek volume (5% for Stiffkey) compared with their large contribution to the total channel length (33% for Stiffkey): we considered it more important to accurately extract the length rather than the width of terminal channels. The generation of straight repair paths may also underestimate channel sinuosity, but here again the error was considered negligible since terminal channels have been found by previous studies to have a sinuosity ratio close to 1 (Steel, 1996).

The reconnection algorithm is only efficient if the creek network is the only significant low-elevation feature: otherwise elements such as ponds or agricultural trenches could be erroneously connected to the creek network. Such features can be removed from the black and white image by adding a feature size filter, which requires further sensitivity tests to ascertain the size of the unwanted features. Other creek repair operations include infilling holes in the creek mask, and spur removal to smooth out the creek contours.

The creek mask gives the total area and, combined with the elevation data from lidar, the volume of the channel network measured from the top of the creek edges (Fig. 6C). The latter constitutes the potential semi-diurnal tidal prism as defined by Steel (1996). Once the creek area mask is complete, morphological thinning is applied to shrink the creek network to a skeleton corresponding to the centerline of the channels (Step 3, Fig. 4). Though different from the thalweg, since the skeleton will be traced in the middle of each creek without necessarily matching the maximal depth point, this method gives an accurate representation of the shape and size of each creek segment (Fig. 6D).

4.2.3. Parameter extraction

Once the creek network shape and skeleton have been defined, the following steps of the algorithm provide quantitative parameters to describe its morphology. The composition and complexity of the creek network can be expressed quantitatively in terms of stream order. Several ordering systems exist, the most commonly used being the Strahler order. In this system, all terminal segments are assigned the order 1; when two segments of the same order meet, their confluence stream is one order higher, and so on (Strahler, 1957). The Strahler ordering system's utility is based on the premise that the order number is proportional to the catchment area and to the creek network dimensions (Strahler, 1957).

This ordering system can be automatically computed using a pruning process. The algorithm detects the end points of the network and assigns the lowest Strahler order 1 to all segments from the end points to their nearest branch point. The selected segments are then removed and the process is repeated, assigning a Strahler order iteratively to all creek segments (Step 4, Fig. 6E). In order to distinguish the entry channel from the small terminal creeks, all end points are assigned a depth corresponding by the mean depth over a 10 pixels window, and the segment connected to the deepest end point is automatically detected as the outlet and assigned the highest Strahler order at the end of the pruning process.

While fully automatic in dendritic systems, the pruning process is halted by the presence of interconnected creeks (Fig. 6E). Previous studies have circumvented this issue by only selecting creek systems that do not branch out in the downstream direction (Novakowski et al., 2004), but our algorithm should be able to monitor MR creek networks,

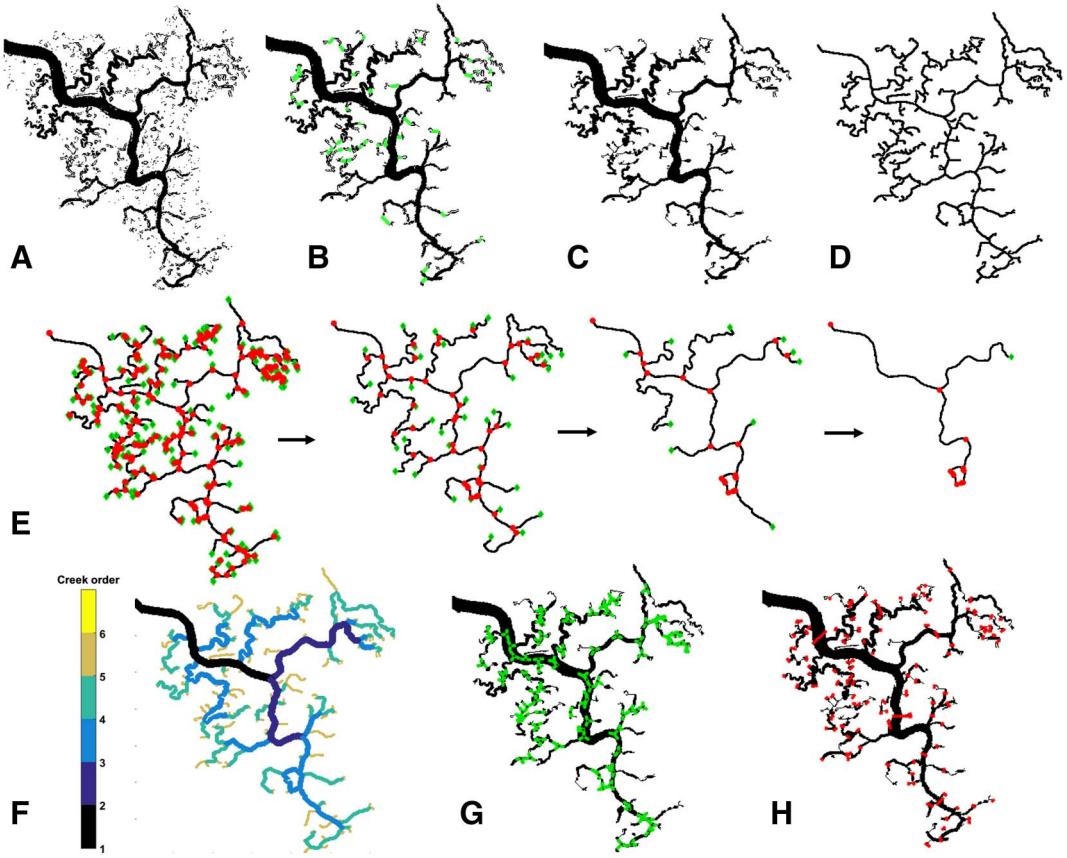

Fig. 6. Creek network repair and parametrization steps applied to Stiffkey Marsh. A: disconnected, noisy creek network mask extracted using elevation and slope thresholds (Step 1). B: creek segments reconnection using shortest Euclidean distance, with repair paths shown in green (Step 2). C: repaired creek mask (Step 2). D: creek skeleton (Step 3). E: pruning process used to assign a Strahler order to the creek segments (Step 4). Green diamonds correspond to end points and red dots to branch points. Terminal segments removed on first iteration are assigned the Strahler order 1, *etc*. In the case of interconnected segments, the Strahler order is assigned manually (Step 5, UI 4). F: Reverse Strahler order (Step 6). G: junction angle, defined as the minimum of the three angles at each channel junction, measured at 0.2 times the mean length of second Strahler order creeks, shown in green (Step 6). H: Creek cross-section across the middle of each segment and delimited by the creek mask, used to calculate the channel width, depth and cross-sectional area, shown in red (Step 6). (For interpretation of the references to color in this figure legend, the reader is referred to the web version of this article.)

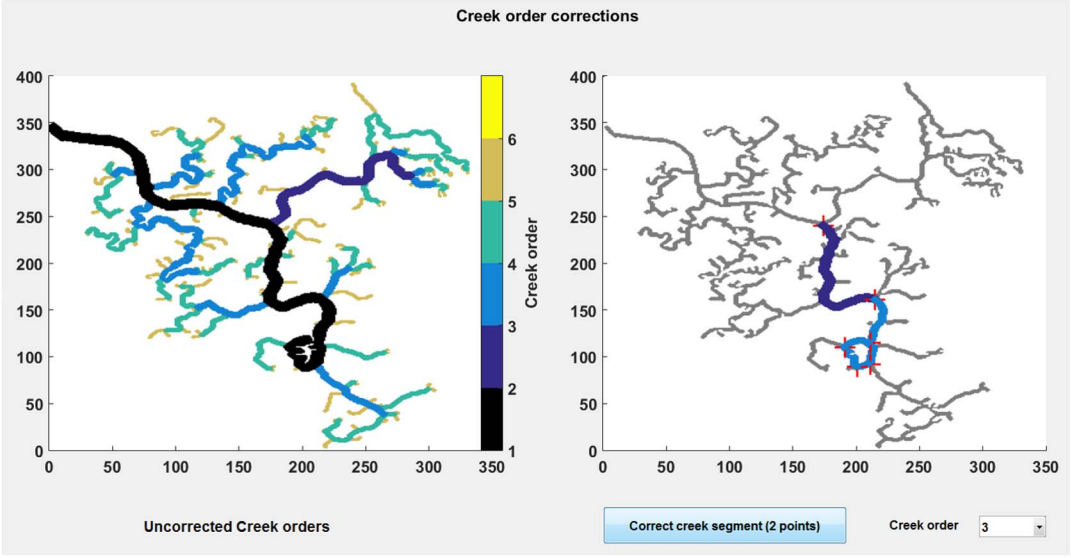

Fig. 7. Creek order correction using an interactive user interface (Step 5, UI 4, Fig. 4). The correct order is selected in a drop-down menu. Segments are then corrected by clicking twice on the right-hand map (red plus signs). (For interpretation of the references to color in this figure legend, the reader is referred to the web version of this article.)

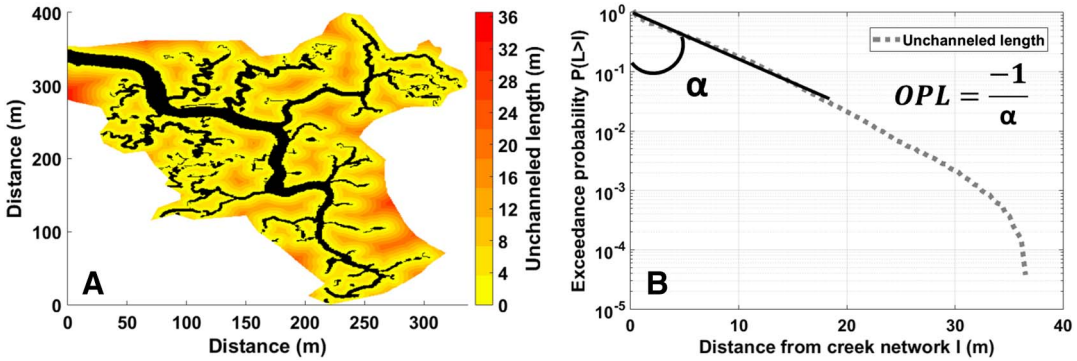

Fig. 8. Illustration of the unchanneled length distribution (A–B) and overmarsh path length OPL (B) at Stiffkey. OPL is the slope of the first 50 values of the exceedance probability distribution in meters, given by $-1/\alpha$ with α the first regression coefficient of the linear fit.

which are typically highly interconnected (Pontee, 2003). A new user input is therefore necessary: erroneous creeks are assigned their correct order manually using an interactive user interface (Step 5, UI 4, Fig. 3, Fig. 7) to get the final creek order map (Fig. 6F).

For each segment, the following parameters are automatically extracted (Step 6, Fig. 4): (1) the channel length — the quasi-euclidean geodesic distance using the Matlab function *bwdistgeodesic*; (2) the sinuosity ratio - the sinuous distance divided by the straight quasi-euclidean distance; and (3) the junction angle — defined as the minimum of the three existing angles at each channel junction, measured at 0.2 times the mean length of second Strahler order creeks following Steel's (1996) method (Fig. 6G). Furthermore, a cross-section of the creek mask obtained in Step 2 (Fig. 4) is taken across the middle of each segment to obtain the channel width, maximal detected depth in the cross-section, and cross-sectional area (Fig. 6H). In addition, the main channel length is measured using the geodesic distance function along the longest channel in each creek network, connecting the mouth to the furthest terminal channel.

Finally, the Strahler order of every creek segment is reversed so that the entry channel becomes the first order, and the terminal channels the highest order (Fig. 6F). The Strahler ordering system's main limitation for saltmarsh restoration studies is that the order of the entry channel appears to change over time as new, smaller channels develop (Weishar et al., 2005). Referring to the entry channel as the first order channel avoids such confusion. The reverse Strahler order was first proposed to study dendritic outgrowth at different stages of development (Uylings et al., 1975). This approach is well suited to the analysis of MR creek network evolution, where the highest order is expected to increase over time as the network expands.

4.3. Predictive value of morphological equilibrium relationships

To fulfill our first objective, this algorithm was tested on the 13 natural saltmarshes presented in Section 3. Using the parameters obtained as outputs, we then estimated the predictive value of existing morphological equilibrium relationships in pursuit of our second objective. To that end, two statistical methods were used: the determination coefficient R^2 provides a measure of the scatter of points about the best fit regression line, and the mean absolute percentage error (MAPE) is an unbiased measure of the predictive value of a model used in hydrological studies (Wang et al., 2009b), commonly defined as:

$$[1]\ \mathbf{MAPE} = \frac{1}{n}\sum_{i=1}^{n}\left|\frac{X_p(i) - X_m(i)}{X_m(i)}\right|^{*} 100$$

With X_m the measured parameter at equilibrium, X_p the parameter at equilibrium as predicted by the power law relationship being tested, and n the number of sites.

4.4. Distribution/drainage efficiency

Though giving information on the size and volume of the channels, the existing morphological relationships mentioned so far gave no information regarding the distribution of the creek system across the site. In order to fulfill the third objective of this paper, we sought to develop new morphological equilibrium relationships using a proxy of the creek network's spatial distribution. This proxy should be representative of the creek network's efficiency at draining the site during the ebb and at distributing water and sediment during the flood tide.

A commonly used proxy is the drainage density, defined by Steel (1996) as the ratio of total channel length *versus* catchment area. This is a one-dimensional metric that gives some information on the creek density, but does not account for spatial distribution (Marani et al., 2003). A more accurate representation of the creek network drainage efficiency is the unchanneled length, the hillslope distance of all pixels to the creek network (Lohani et al., 2006; D'Alpaos et al., 2007; Kearney and Fagherazzi, 2016). Flat distance was used in this paper instead of 3D distance over the sloping surface to reduce computation time, and because the elevation gradient is generally very low in intertidal wetlands (Table 1). This parameter is a morphological approximation of the hydrodynamic-based measures of flow paths (Marani et al., 2003), and is more useful than drainage density for describing ecosystems, as vegetation distribution is correlated with the distance to the creek network (Temmerman et al., 2005).

The unchanneled length is plotted as a semi-logarithmic exceedance probability distribution curve showing the distance to the creek network for each pixel in the DSM (Fig. 8A). The drainage efficiency of the creek network can also be expressed quantitatively using the Overmarsh Path Length (OPL), the slope of the first 50 values of the exceedance probability distribution in meters, given by $-1/\alpha$ with α the first regression coefficient of the linear fit (Fig. 8B). OPL gives the average distance that needs to be crossed within a marsh before encountering a creek: the lower this parameter, the better irrigated the site by a dense and well-distributed creek system (Marani et al., 2003), while a marsh characterized by a large OPL is “emptier”.

We related OPL to the initial morphological conditions and tidal forcings through a multiple linear correlation, and verified the proportionality of OPL with the catchment area. In order to select, among the available variables, which accounted for most of the variability in the dataset, a principal component analysis (PCA) was performed. PCA reduces the dimensionality of the dataset while retaining as much of the variation as possible (Jolliffe, 2002). This is done by transforming the variables into a new set of uncorrelated principal components (PC), where the first few PCs contain most of the variation in the original variables. One limit of PCA is that it assumes all variables are normally distributed, a condition that was not necessarily met in our case. However, useful descriptive information can be inferred from PCA in terms of classification of intercorrelated parameters even if the data are

Table 2
List of parameters selected for PCA due to their relevance to creek design and evolution.

Parameters selected for PCA	Relevance to creek design
Catchment area (m^2)	Morphological markers of creek development already used in equilibrium relationships (group 1)
Main channel cross-sectional area (m^2)	
Main channel depth (m)	
Main Channel length (m)	
Main channel width (m)	
Total channel length (m)	
Total creek volume (potential tidal prism) (m^3)	
Drainage density (m/m^2)	Markers of creek drainage efficiency (group 2)
Overmarsh path length (OPL) (m)	
Mean marsh elevation above mean spring sea level (m)	Tidal forcings (group 3)
MSTR (mean spring tidal range) (m)	
Tidal asymmetry (flood duration/ebb duration)	
Main channel gradient (°)	Markers of creek maturity (group 4)
Marsh age (years)	
Mean sinuosity ratio	
< 20 μm sediment %	Marker of sediment stability (group 5)

not normally distributed (Jolliffe, 2002).

The choice of variables included in the PCA was guided mainly by the need to produce a tool to help future MR design. This justifies the use of a limited number of parameters: designers tend to have limited access to information on the vegetation distribution or sediment properties, especially since those properties may change post-implementation with new sediment being brought to the system. Another limitation of PCA is the assumption that the variables selected fully represent the statistical variation of the dataset (Steel, 1996; Jolliffe, 2002). In this study, we operated with a limited set of parameters, so the interpretations inferred should be treated with caution, but graphical observation of the PCs can provide some indication of the relative importance of each considered variable.

We separated the selected parameters into 5 groups (Table 2): morphological markers of creek development already used in equilibrium relationships; markers of creek drainage efficiency; tidal forcings; markers of creek maturity corresponding to phase D of marsh development (Fig. 1) where the system is at equilibrium with a low channel gradient and a sinuous creek network; and markers of sediment stability given by the percentage of cohesive sediment. All variables were standardized by subtracting the mean and dividing by the standard deviation in order to account for the effects of scale and different units (length, area, volume, time). We ran the PCA expecting all groups to stay together in the PCs as they should be intercorrelated. Of particular interest was to which group the drainage efficiency (group 2) would be most closely correlated: to other morphological characteristics, to the tidal forcings, to the maturity of the system or to the sediment stability?

The first three PCs accounted for over 75% of the dataset variance, making them sufficiently representative of the variability of the dataset [Stevens, 1986 cited in Steel, 1996]. The classification into independent PCs helped to pick variables for the multiple linear regression, and to propose a morphological equilibrium relationship using the drainage efficiency represented by OPL. We used the Matlab function *fitlm* to create a linear regression model, and the function *step* to automatically add or remove variables to optimize the fit. This iterative process is efficient for the relatively small number of variables considered here. The best fit obtained gave out a new morphological equilibrium relationship to fulfill objective 3.

5. Results

5.1. Creek network parametrization algorithm performance compared with field-based survey

This section fulfills objective 1 by evaluating the performance of our semi-automated creek parametrization algorithm. We compared the creek networks yielded by our algorithm with networks extracted manually by Steel (1996) (Fig. 9). Our algorithm successfully captured the variety in width and sinuosity of the low reverse order channels. For example, the entry channel of the Tollesbury marsh is noticeably wider and more sinuous than the others, while the Banks marsh displays a thin entry channel compared to the other sites (Fig. 9B). Some fusing of high reverse order channels caused an overestimation of the creek width (See Grange marsh, Fig. 9B). In other places, the creek network repair algorithm produced very thin channels (visible for Tollesbury) to limit channel interconnection, as explained in Section 4.2.3. Many of the high reverse order channels drawn by Steel (1996) were not detected with our method, especially in complex systems like Grange Marsh (Fig. 9A and C). However, the shape of the larger channels and the extent of the creek network matched well with Steel's results.

All segments were given a reverse Strahler order for better representation of the creek network branching complexity. This complexity is greater at Tollesbury, where the creeks are highly sinuous and sometimes interconnected, than at Banks (Fig. 10). Mean morphological parameters were extracted for each reverse order and plotted against Steel's (1996) results (Fig. 11). We observed an exponential increase of the number of creek segments with reverse order, associated with an exponential decrease in creek segment length, depth and cross-sectional area (Fig. 11A–D). The differences between our results and Steel's (1996) were less than an order of magnitude. The depth of channels measured using lidar were up to 0.5 m shallower than Steel's field validated results (Fig. 11C), probably due to the presence of residual water at the bottom of most creeks: this is a limitation of using near infrared lidar data which cannot penetrate water (Brzank et al., 2008). As a result, and because creek width is overestimated when adjacent creeks are detected as one channel due to the resolution of the dataset, the width/depth ratio was systematically overestimated by the extraction algorithm (Fig. 11E). Even though the values fell within those expected of intertidal creek networks, between 5 and 34 (Zeff, 1999), no correlation could be found between the width/depth ratio and the reverse order. However, in the case of the cross-sectional area and the mean width value given by the area/depth ratio in m (Fig. 11D and F), the depth underestimation had a much lower impact, and the results are close to Steel's (1996), with higher values for first reverse order channels. The sinuosity ratio yielded similar results to Steel's (Fig. 11G): the first reverse order channels displayed a range of sinuosity values between 1 and 1.6, and creeks became more uniformly straight with increased reverse order. The mean bifurcation ratio of the higher reverse order channels ranged between 3.0 and 5.2, with a mean value of 3.70 (Fig. 11H), meaning that this algorithm detected on average 3.7 times more creeks for each new reverse order.

5.2. Applicability of morphological relationships

In order to fulfill objective 2, morphological relationships currently proposed to guide MR design (Steel, 1996; Williams et al., 2002; Marani et al., 2003) were re-tested using the parameters obtained from the semi-automated extraction algorithm. Similar relationships were obtained, with correlation coefficients $R > 0.60$ and determination coefficients R^2 comprised between 0.38 and 0.79 (Fig. 12, Table 3). The largest discrepancies between Steel's (1996) and the present study's equilibrium relationships' coefficients were the ones relating the creek mouth width to the tidal prism and to the total channel length.

The predictive value of each relationship was approximated by the mean absolute percentage error MAPE (Table 4). MAPE results were

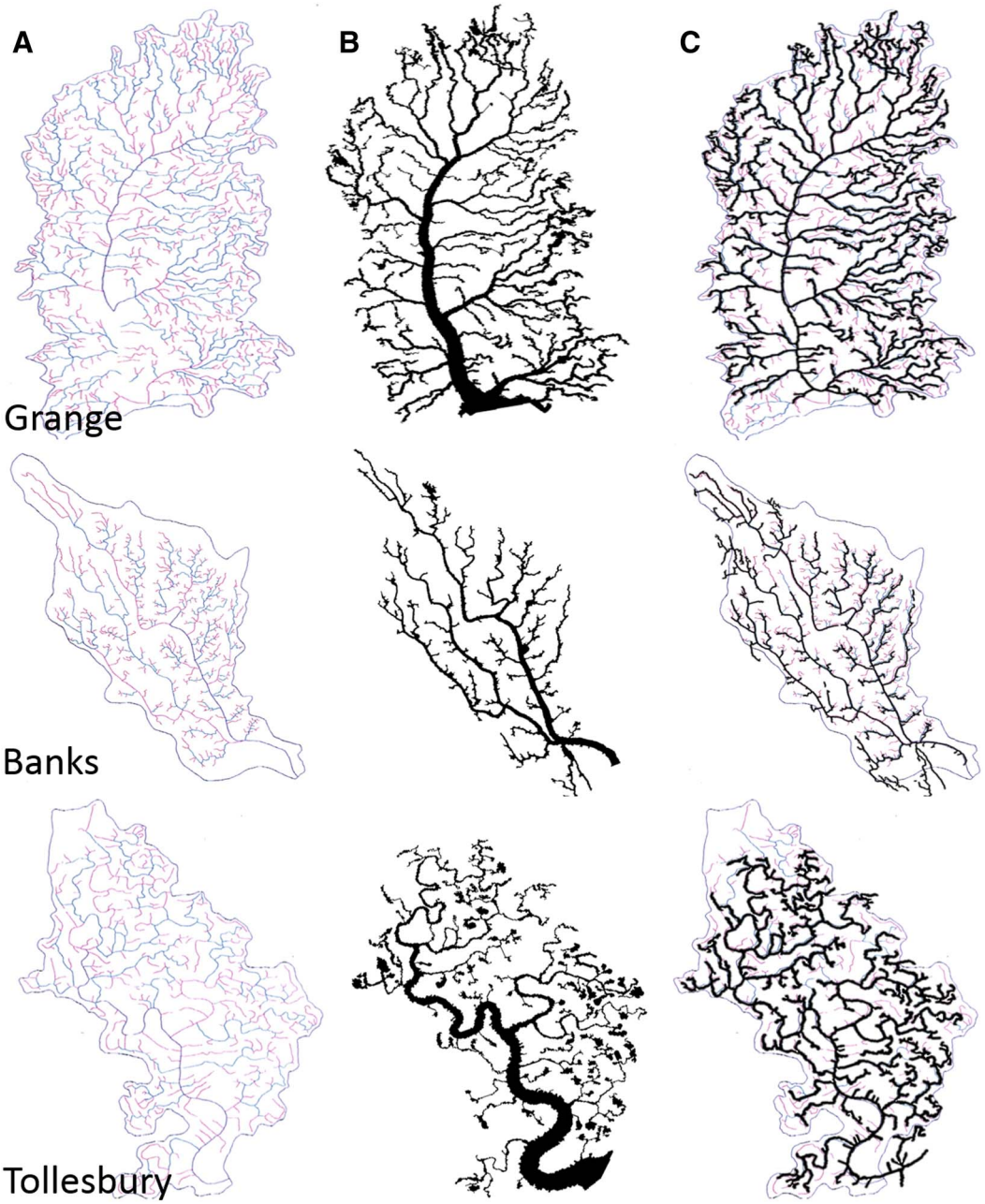

Fig. 9. Creek area and skeleton extraction results from three out of thirteen saltmarshes, compared with Steel's channel extraction results (1996). A: Creek network skeleton manually extracted by Steel. B: creek mask. C: creek skeleton overlain over Steel's manual extraction results.

over 25% for all morphological relationships tested. MAPE was higher for the total channel length, because the number of channels detected depends on the resolution of the dataset, and on the channel width due to the extraction error discussed in Section 4.2.2. Yet, even though Steel's (1996) relationships predicted higher depth values and lower width values compared to the lidar results, both projections lie within the spread of the measured data (Fig. 13C–D). The main and total channel lengths were well represented by both relationships (Fig. 13A–B). Finally, MAPE was higher for the cross-sectional *versus* main channel catchment area than *versus* tidal prism or total channel length. This suggests that catchment area is an imperfect predictor of the main channel cross-sectional area at equilibrium.

5.3. Creek network drainage efficiency

The unchanneled length shows the distance to the creek network at each point of the saltmarsh, and allows us to calculate the overmarsh path length (OPL) as explained in section 4.3. In order to fulfill the third objective of this paper, we defined an equilibrium relationship relating OPL to initial morphological conditions and tidal forcing.

An exponential decay of the unchanneled length exceedance probability distribution was observed, in accordance with results from Marani et al. (2003), with faster collapsing curves corresponding to the better drained saltmarshes (Fig. 14A). We found no sign of proportionality between OPL and the catchment area or tidal prism. For example, Warren Farm and Grange had similar distance distributions to the creek network despite the difference in size (Table 1, Fig. 14A). The maximum unchanneled length remained below 100 m and OPL between 3 and 25 m, except for Crossens and Gibraltar Point, which were poorly drained as shown by the comparison of Grange Marsh and Gibraltar Point (Fig. 14B–C). Crossens and Gibraltar Point are both younger than the other saltmarshes studied by Steel (1996) (Table 1),

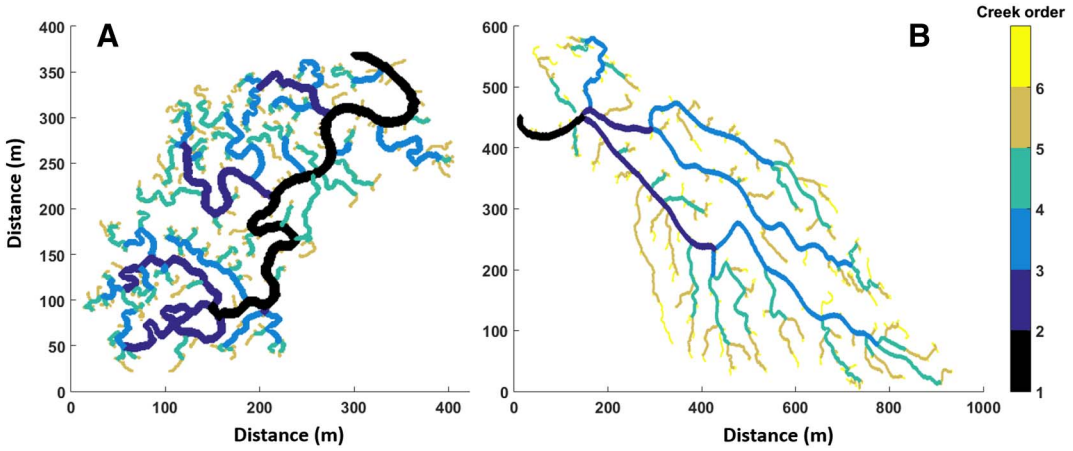

Fig. 10. Reverse Strahler order of creek segments in Tollesbury Marsh (A) and Banks Marsh (B).

but age is not enough to explain the stark difference in creek network extent. Indeed four sites, Tir Morfa, Hen Hafod, Portbury Wharf and Shell Ness, which were estimated by Steel (1996) to be 50 years old or less when their creek network was first mapped (Table 1), do not display the underdeveloped creek network visible at Crossens and Gibraltar Point (Fig. 14A). Other unexplained factors either have prevented the creek network development of Gibraltar Point and Crossens, or accelerated the development of the four other sites. In any case, Crossens and Gibraltar Point were considered to be out of equilibrium and removed from the PCA.

The PCA gave out the contribution of each selected variable to the first three PCs, which cumulatively accounted for 78% of the total variability of the dataset (Table 5). We also used a three-dimensional biplot to visually interpret the relationships between the variables (Fig. 15). Due to missing parameters relevant to the development of saltmarshes (vegetation, flow velocity, number of flooding events per year), PCs were hard to interpret beyond the third component. Input variables were separated into the three PCs based on their highest absolute loadings.

Principal Component 1 was dominated by size-related variables, as is typical of a first PCA component (Steel, 1996). Group 1 variables identified in Table 2 were all positively correlated (Fig. 15A) in agreement with traditional morphological equilibrium relationships for creek networks. They displayed similar loading values between 0.33 and 0.37 (Table 5), suggesting that they all have similar weights as a proxy of the creek network size.

Principal Component 2 related the tidal forcings (group 2) and the markers of drainage efficiency (group 3). This suggests that the drainage efficiency of a saltmarsh at equilibrium depends more on the tidal forcings than on morphological features such as the dimensions of the main channel (group 1). A well distributed creek network, characterized by a low OPL and a high drainage density, is associated with a low MSTR, a high tidal asymmetry, and critically by a low elevation above MWS. Indeed, the higher the site within the tidal frame, the fewer flooding events will reach the saltmarsh, reducing both the hydrodynamic energy and the sediment supply. This can hinder creek network development or even cause its contraction as seen in the conceptual model, thus reducing the drainage efficiency (Fig. 1).

Finally, Principal Component 3 related the creek maturity variables (group 4) with the sediment stability (group 5). Higher concentration in cohesive material restricts the growth of the creek system by increasing the stability of the channels against erosion (Steel, 1996), which leads to lower creek sinuosity even in older marshes. This seems an accurate representation of controls on channel sinuosity, if simplistic: in saltmarshes, the channel sinuosity will also depend on flow conditions and vegetation cover (Zeff, 1999).

The PCA analysis facilitated the selection of variables for a multiple linear regression and allowed us to propose morphological equilibrium relationships using OPL. The best relationship found related OPL with two independent variables: the elevation within the tidal frame and the mouth cross-sectional area (Eq. [21], Fig. 16A). The MAPE is 50.6% and the determination coefficient $R^2 = 0.80$ (Fig. 16A). Another statistically significant relationship was found between OPL and the elevation within the tidal frame (Eq. [22], Fig. 16A).

6. Discussion

The first objective of this paper was to test the efficiency of our new creek parametrization algorithm using lidar data, by comparing our results with those from previously studied creeks. We used a semi-automated algorithm based on the threshold method. The creek detection criteria are intuitive and in accordance with most previous studies: a creek network is defined as a connected feature which lies lower than the rest of the saltmarsh, and whose edges are delimited by a steeper slope. Those criteria are strictly based on morphology rather than as a function of runoff like the D8 flow accumulation method (James and Hunt, 2010) and are thus well suited to the study of both natural and artificial creek networks.

The method is semi-automated with only a few user inputs needed, such as choosing the elevation and slope thresholds values and choosing the noise threshold to filter isolated features during the creek repair phase (Fig. 4). The elevation and slope thresholds are estimated visually by inspecting distribution curves and then optimized by trial and error. The time required to obtain the creek maps and parameter tables for a 500,000-pixel dataset containing a complex sixth order creek network is only 80 s on a standard desktop computer, making this a much faster method than slow and labour-intensive manual digitization from aerial photographs (Mason et al., 2006). This also facilitates running a large number of sensitivity tests for each site, using different thresholds to optimize the output creek network. Another advantage is that consistent morphological criteria are used to detect creeks, rather than subjective visual interpretation: the latter method can be a source of error in studies that do not ground-truth their extracted creeks with field surveys, as creeks of an order of 1 cm depth can be clearly visible in aerial photography, despite having no significant influence on water distribution and drainage.

The method developed herein yielded realistic creek network shapes for all 13 studied sites when compared with field validated results (Fig. 9). The preprocessing phase was minimal, which avoided loss of data through smoothing. Most of the errors observed, such as the underestimation channel depth, could be retraced to data collection, such as the reflection or absorption of the laser beam by residual water in the channels (Mason et al., 2006).

Our creek extraction algorithm is also the first to yield as outputs a

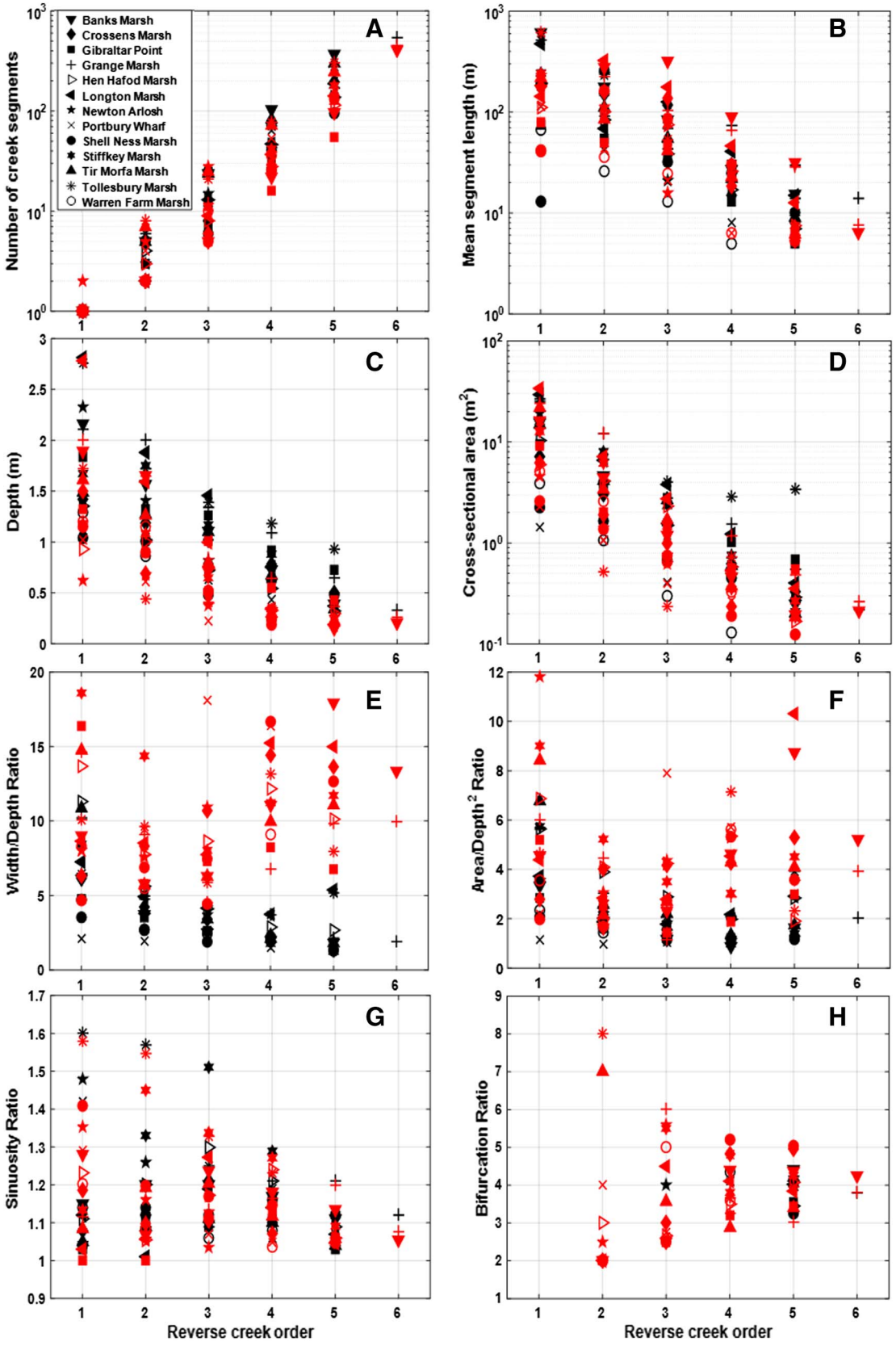

Fig. 11. Morphological characteristics per reverse Strahler order as identified by Steel, 1996 (black) and by the semi-automated extraction algorithm (red). A: magnitude; B: mean length; C: maximal depth; D: cross-sectional area; E: width/depth ratio; F: area/depth^2 ratio (mean width/depth ratio); G: mean sinuosity; H: bifurcation ratio. (For interpretation of the references to color in this figure legend, the reader is referred to the web version of this article.)

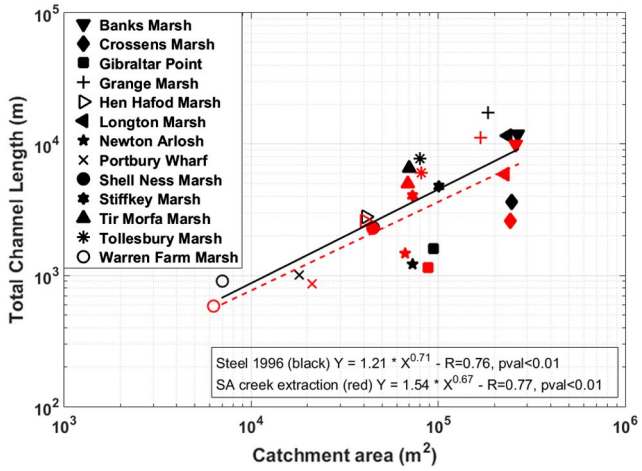

Fig. 12. Correlation between the total channel length (m) and the catchment area (m^2) using Steel's data (1996) in black and the results from the semi-automated (SA) creek extraction algorithm in red. (For interpretation of the references to color in this figure legend, the reader is referred to the web version of this article.)

comprehensive suite of morphological parameters for each creek order. We found an exponential increase in creek number and decrease in creek length with increasing reverse order (Fig. 11A–B), in agreement with the laws of drainage composition established by Horton (1945) on fluvial networks and with previous studies on intertidal creek network compositions (Steel, 1996; Zeff, 1999). Consequently, our algorithm could be used to monitor saltmarsh restoration sites to verify the creek system's compliance with natural drainage compositions, as well as for monitoring rapidly evolving natural systems under the influence for instance of subsidence or sea level rise (Marani et al., 2003).

Other automated methods have been developed recently based on an eight direction enhancement and detection of Gaussian shapes to extract creek networks (Liu et al., 2015). Their results outperformed the traditional threshold methods in the case of a tidal creek network covering an area of 5,000 km^2, for creek networks as small as 5 m wide. However, the applicability of this method to artificial creek networks, which are not always characterized by Gaussian-shaped cross-section profiles like natural channels, is unclear. An interesting extension of this work would be to apply their method to the 13 British saltmarshes used here, and verify whether a similar creek network is obtained to try and reduce the error in channel width extraction observed in our results (Fig. 11E) by yielding more accurate and objective creek edges, rather than relying on sensitivity tests. A notable advantage of our proposed algorithm is that, while the creek detection relies on traditional threshold methods, the more novel creek parametrization phase can be applied to the output of other creek extraction techniques, as long as they provide a connected creek mask.

The second objective of this paper was to determine the applicability of existing morphological equilibrium relationships to lidar-extracted data. In Steel's (1996) study, the creeks mapped were validated during field surveys as being all deeper than 0.2 m and longer than 2 m. Given the 0.15 m vertical and 1 m horizontal resolution of our lidar datasets, the smallest features that could be reliably identified were channels of 2 m length, 2 m width, and 0.3 m depth. Furthermore, channels < 2 m apart often appeared fused in the lidar data. These resolution limits were identified as the cause for the small errors of omission observed when comparing our results with Steel's (1996) for both the creek number and creek length (Fig. 9). Yet, despite those omissions, our algorithm accurately detected the creek system composition, even though the development phase of the creek network may be underestimated due to the resolution used.

We interpreted the systematic depth underestimation as an error inherent to lidar data collection, as the laser does not penetrate water (Brzank et al., 2008). The width of creeks was overestimated when adjacent creeks were fused due to the resolution of the dataset, causing the width/depth ratio to be systematically overestimated (Fig. 11E). Using the area/depth ratio as an approximation of the mean segment width lowered the impact of width overestimation and gave closer results of mean width/depth ratio to those found by Steel (1996) (Fig. 11F). As some MR schemes guidelines recommend reproducing the width/depth ratios of similar natural systems (Zeff, 1999), when monitoring the channel shape we recommend using the mean width/depth ratio given by area/$depth^2$ to lessen the error associated with creek width detection in 1 m resolution lidar data.

The relationships were also qualitatively in accordance with those established in previous studies using aerial photography and field surveys in the Venice lagoon (Marani et al., 2003) and San Francisco Bay (Williams et al., 2002). However, the MAPE was over 25% for all morphological relationships tested. This is due to the inherent variability of creek network shapes, and implies that the morphological relationships are not effective in quantitatively predicting the final shape of the creek network based on the initial conditions. They can, however, provide semi-quantitative trends suggesting how design choices may accelerate or hinder evolution towards equilibrium. This will be done in our upcoming study of MR sites, where these relationships will be used to determine how close to morphological equilibrium creek networks in current MR schemes have gotten after up to 20 years of evolution. By determining rates of evolution of these sites towards equilibrium, and comparing those rates to the initial design choices, we will be able to provide new design guidelines for MR creek networks to address the current lack of systematic design strategies.

Considering this limitation, the predictive value of the

Table 3
Determination coefficients of morphological equilibrium relationships of the creek network in natural saltmarshes established by Steel (1996) and the present study.

Parameters (y *vs.* x)	Steel's relationship (Steel, 1996)	R^2 (Steel, 1996)	Creek extraction relationship (present study)	R^2 *p*-value
Total channel length (m) *vs.* catchment area (m^2)	$y = 1.7 \times^{0.7}$	0.57	$y = 1.5 \times^{0.7}$	$R^2 = 0.59$ $p < 0.01$
Maximum creek mouth width (m) *vs.* potential semi-diurnal tidal prism (m^3)	$y = 0.28 \times^{0.4}$	0.69	$y = 0.7 \times^{0.4}$	$R^2 = 0.49$ $p = 0.01$
Main creek length (m) *vs.* catchment area (m^2)	$y = 1.5 \times^{0.5}$	0.70	$y = 1.6 \times^{0.5}$	$R^2 = 0.71$ $p < 0.01$
Maximum creek mouth width (m) *vs.* total channel length (m)	$y = 0.22 \times^{0.5}$	0.46	$y = 0.61 \times^{0.4}$	$R^2 = 0.38$ $p = 0.03$
Mean cross-sectional area of main creek (m^2) *vs.* total channel length (m)	$y = 0.04 \times^{0.7}$	0.46	$y = 0.03 \times^{0.7}$	$R^2 = 0.61$ $p < 0.01$
Mean cross-sectional area of main creek (m^2) *vs.* catchment area (m^2)	$y = 0.01 \times^{0.6}$	0.48	$y = 0.03 \times^{0.5}$	$R^2 = 0.41$ $p = 0.02$
Mouth cross-sectional area of main creek (m^2) *vs.* potential semi-diurnal tidal prism (m^3)	$y = 0.02 \times^{0.7}$	0.80	$y = 0.04 \times^{0.7}$	$R^2 = 0.79$ $p < 0.01$

Table 4
Mean absolute percentage error (MAPE) expressed in percentage showing the predictive value of the 19 considered equilibrium relationships. Relationships are shown in white and marked [A] for the present study, light grey for Steel's (1996) study [B], and dark grey for Marani et al.'s (2003) [C] and Williams et al.'s (2002) [D] studies. Note that Williams et al.'s (2002) relationships express the catchment area in ha and not m^2.

Parameters (y *vs.* x)	Relationship	Origin	MAPE (%)
Total channel length (m) *vs.* catchment area (m^2)	[2] $y = 1.7 \times^{0.7}$	British saltmarshes [A]	86
	[3] $y = 1.5 \times^{0.7}$	British saltmarshes [B]	54
	[4] $y = 0.02 \times$	Venice lagoon saltmarshes [C]	58
Main creek length (m) *vs.* catchment area (m^2)	[5] $y = 1.5 \times^{0.5}$	British saltmarshes [A]	38
	[6] $y = 1.6 \times^{0.5}$	British saltmarshes [B]	34
Maximum creek mouth width (m) *vs.* potential semi-diurnal tidal prism (m^3)	[7] $y = 0.28 \times^{0.4}$	British saltmarshes [A]	53
	[8] $y = 0.7 \times^{0.4}$	British saltmarshes [B]	34
Maximum creek mouth width (m) *vs.* catchment area (m^2)	[9] $y = 3.44 \times^{0.552}$	San Francisco Bay coastal saltmarshes [D]	53
Maximum creek mouth width (m) *vs.* total channel length (m)	[10] $y = 0.22 \times^{0.5}$	British saltmarshes [A]	39
	[11] $y = 0.61 \times^{0.4}$	British saltmarshes [B]	37
Main channel depth (m) *vs.* catchment area (ha)	[12] $y = 0.91 \times^{0.21}$	British saltmarshes [B]	25
	[13] $y = 1.31 \times^{0.202}$	San Francisco Bay coastal saltmarshes [D]	53
Mean cross-sectional area of main creek (m^2) *vs.* total channel length (m)	[14] $y = 0.04 \times^{0.7}$	British saltmarshes [A]	31
	[15] $y = 0.03 \times^{0.7}$	British saltmarshes [B]	30
Mean cross-sectional area of main creek (m^2) *vs.* catchment area (m^2)	[16] $y = 0.01 \times^{0.6}$	British saltmarshes [A]	60
	[17] $y = 0.03 \times^{0.5}$	British saltmarshes [B]	59
Mean cross-sectional area of main creek (m^2) *vs.* catchment area (ha)	[18] $y = 2.4 \times^{0.772}$	San Francisco Bay coastal saltmarshes [D]	85
Mouth cross-sectional area (m^2) *vs.* potential semi-diurnal tidal prism (m^3)	[19] $y = 0.02 \times^{0.7}$	British saltmarshes [A]	60
	[20] $y = 0.04 \times^{0.66}$	British saltmarshes [B]	30

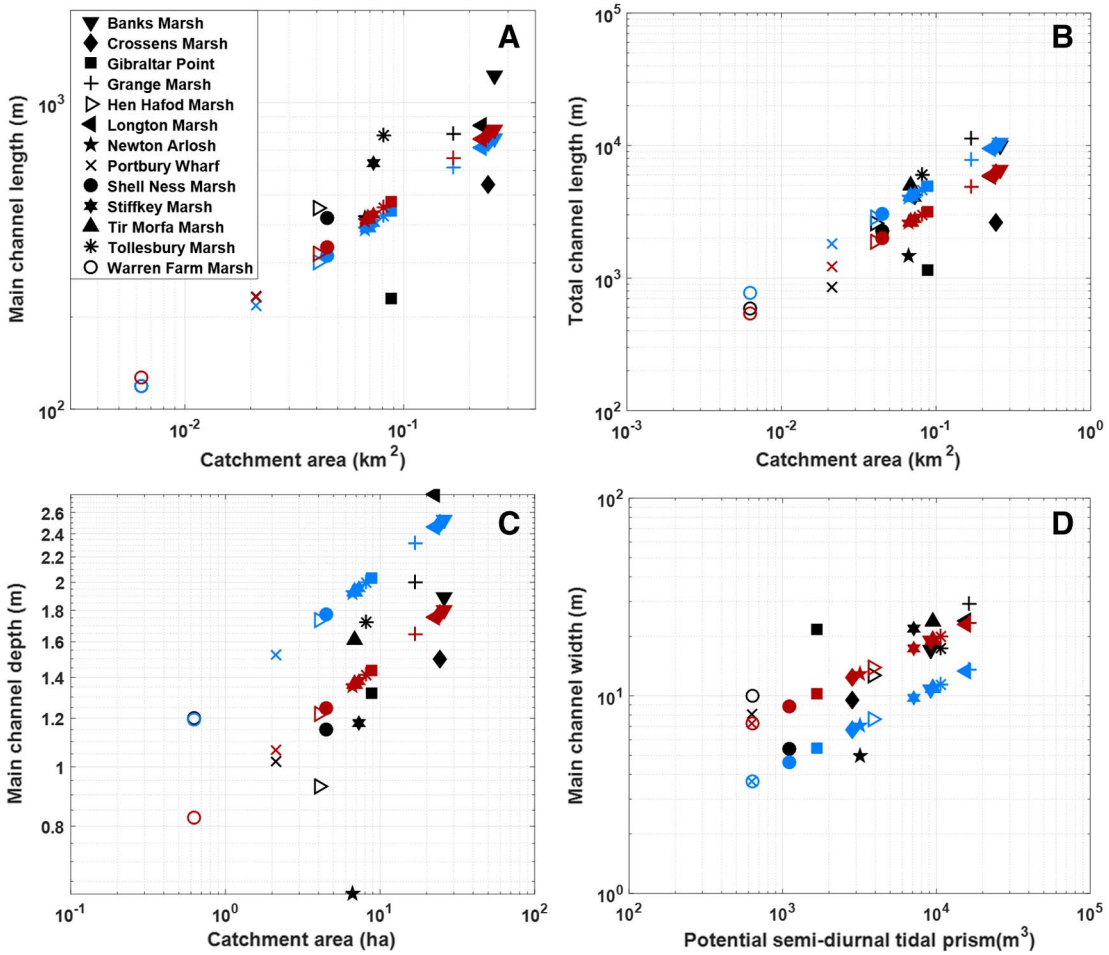

Fig. 13. Representation of the dataset by Steel's (1996) relationships (light blue) and those established from Lidar data on the same coastal saltmarshes (dark red). Lidar measured data in black. A: Main channel length *versus* catchment area. B: Total channel length *versus* catchment area. C: Main channel depth *versus* catchment area (note that Williams et al.'s, 2002 relationships express the catchment area in ha and not m^2). D: Main channel width *versus* potential semi-diurnal tidal prism. (For interpretation of the references to color in this figure legend, the reader is referred to the web version of this article.)

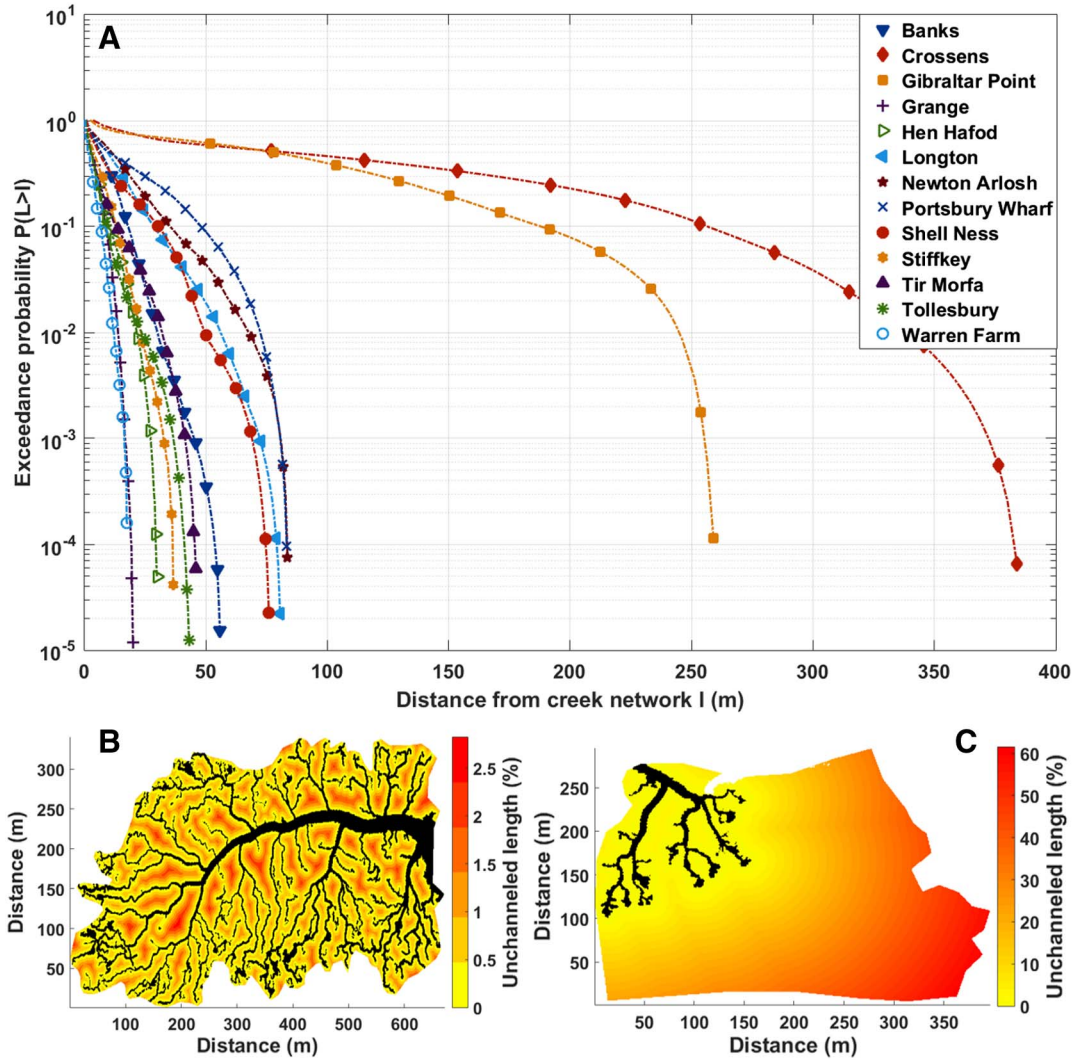

Fig. 14. A: Unchanneled length exceedance probability distribution for all sites in meters (Slope gives the overmarsh path length in meters). B and C: Unchanneled length exceedance probability distribution for Grange (B) and Gibraltar Point (C) expressed as percentage of the major axis length parallel to the main channel.

morphological relationships did not vary significantly with data collection site: the British saltmarshes studied display tidal ranges ranging from mesotidal to hypertidal, and environments ranging from estuarine back-barrier to open coast saltmarshes (Steel, 1996). By contrast, the creek networks analyzed to obtain Eq. [4] in Table 4 were developed in the microtidal environment of the Venice Lagoon (Marani et al., 2003), and those studied to obtain Eqs. [9], [13] and [18] in Table 4 developed in San Francisco Bay under a micro- to mesotidal regime (Williams et al., 2002). The results tend to confirm the hypothesis that those relationships are site-independent (Zedler and Reed, 1995; Marani et al., 2003). This provides further evidence that these relationships can be used for saltmarsh restoration projects around the world.

The morphological relationships we selected to study MR creek network evolution towards equilibrium in our future research are those with a prediction error < 40%, except for relationships involving the channel width, as it is the parameter we extract with the least confidence (Fig. 11D and E). This corresponds to Eqs. [6] (main creek length *versus* catchment area), [12] (maximum creek mouth depth *versus* catchment area), and [20] (Mouth cross-sectional area of main creek *versus* potential semi-diurnal tidal prism) in Table 4. The total channel length *versus* catchment area (Eq. [3], Table 4) will also be used despite its weak predictive value because it is expected to be very sensitive to creek network development (Hampshire, 2011).

The third objective of the paper was to establish a new equilibrium relationship linking the drainage efficiency of the creek network to initial morphological conditions and tidal forcing. The overmarsh path length (OPL), by giving the mean distance to the creeks within the saltmarsh, was found to be a relevant descriptor of drainage efficiency. Interestingly, no correlation was found between OPL and the saltmarsh area. While intuitively larger marshes could be thought to have a greater distance between creeks, the studied natural saltmarshes at equilibrium displayed OPL values ranging between 3 and 25 m, except for the two anomalous sites Crossens and Gibraltar Point. This characteristic is important for plant diversity, as tidal channels have an influence on vegetation within 20 m away from the channel, with a greater plant diversity found within the first 10 m (Sanderson et al., 2000). OPL values significantly over 25 m could be detrimental to saltmarsh plant diversity, and OPL should thus be treated as a critical design factor for MR sites.

In an attempt to guide future design, new equilibrium relationships were found relating OPL with two independent variables: the elevation within the tidal frame and the mouth cross-sectional area (Eqs. [21, 22] Fig. 16). This is in accordance with previous studies stating that marsh elevation within the tidal frame is the main control of the tidal forcing parameters (Reed et al., 1999) and of the sedimentation rates (French, 2006). In terms of MR design, the relationships indicate that the drainage efficiency of the creek network at equilibrium is higher when the scheme is more open to tidal influence (low within the tidal frame with

Table 5
Loadings for the first three principal components, explaining over 75% of the total variation, following PCA applied on standardized variables for all sites except Crossens and Gibraltar Point. Groups of correlated variables are shown in blue for PC1, red for PC2 and black for PC3.

Principal components	1	2	3
Catchment area	**0.352892**	0.140786	0.029925
Main channel cross-sectional area	**0.354785**	−0.00205	0.182986
Main channel depth	**0.331946**	0.03082	0.294776
Main Channel length	**0.347649**	0.03763	−0.13917
Main channel width	**0.33226**	−0.12401	0.140637
Total channel length	**0.353886**	−0.06343	0.082533
Total creek volume (potential tidal prism)	**0.373459**	−0.03729	0.111655
Drainage density	−0.07828	**−0.43337**	0.26119
Overmarsh path length (OPL)	−0.16168	**0.419193**	0.026943
Mean marsh elevation above MWS	−0.01529	**0.4672**	0.189349
MSTR (Mean spring tidal range)	0.015825	**0.454036**	−0.0632
Tidal asymmetry	−0.21557	**−0.29735**	0.254115
Main channel gradient	−0.23902	0.073416	**0.442639**
Marsh age	0.058982	−0.14348	**−0.42326**
Mean sinuosity ratio	0.02527	−0.20428	**−0.39982**
<20μm sediment %	−0.05448	−0.11371	**0.334653**
Explained variation	40.04569	24.6017	13.34988
Cumulative explained variation	42.63125	64.64739	77.99727

a large site opening); this also fits with our PCA results which found the drainage efficiency to be correlated to the tidal forcings (Fig. 15A). The MAPE values for the two equations are lower than for Eq. [3], and with R^2 value of 0.63 and 0.80 respectively, we consider these equations to be suitable tools to assist in the monitoring and design of creek networks in MR schemes. Preliminary testing found Eq. [22] to be more convenient than [21] for MR creek evolution monitoring: indeed, the mouth cross-sectional area in MR schemes generally corresponds to a breach in a seawall, with much greater values than a natural channel outlet, making the creek evolution in relation to Eq. [21] difficult to interpret.

In summary, the efficiency of existing morphological relationships has been tested for lidar-extracted data. A mean prediction error > 25% was found for all morphological relationships tested, showing the inherent variability of saltmarsh creek network shapes, which limits the predictability of their equilibrium state. Morphological relationships can, however, be used to monitor trends of evolution towards equilibrium and determine which initial design choices encourage that evolution. The overmarsh path length (OPL) has been found to be a valid proxy of the drainage efficiency of the creek network, and is a relevant addition to the planimetric parameters already in use to determine morphological equilibrium. The following relationships will be used in further studies on artificial creek networks in MR schemes:

$y = 1.5 \times {}^{0.7}$ Total channel length *vs.* catchment area.

$y = 1.6 \times {}^{0.5}$ Main creek length *vs.* catchment area.

$y = 0.91 \times {}^{0.21}$ Main channel depth *vs.* catchment area.

$y = 0.04 \times {}^{0.66}$ Mouth cross-sectional area *vs.* potential semi-diurnal tidal prism.

$z = 3.64 \times -0.27y$ Overmarsh path length *vs.* marsh elevation within the tidal frame and mouth cross-sectional area.

$y = 3.49 \times -1.03$ Overmarsh path length *vs.* marsh elevation within the tidal frame.

MR schemes designers need advice on creek network design, which the morphological relationships validated in this analysis can provide. However, the applicability of our findings is currently limited by the relatively small number of sites (13) considered. Indeed, our sample was limited to sites where morphological parameters had already been extracted by a field-validated study; the dataset collected by Steel is the most complete in that regard. Still, the relationships were similar to those found in previous studies, which analyzed 12 marshes in San Francisco Bay and 20 marshes in Venice Lagoon, respectively (Williams et al., 2002; Marani et al., 2003), suggesting an applicability of the

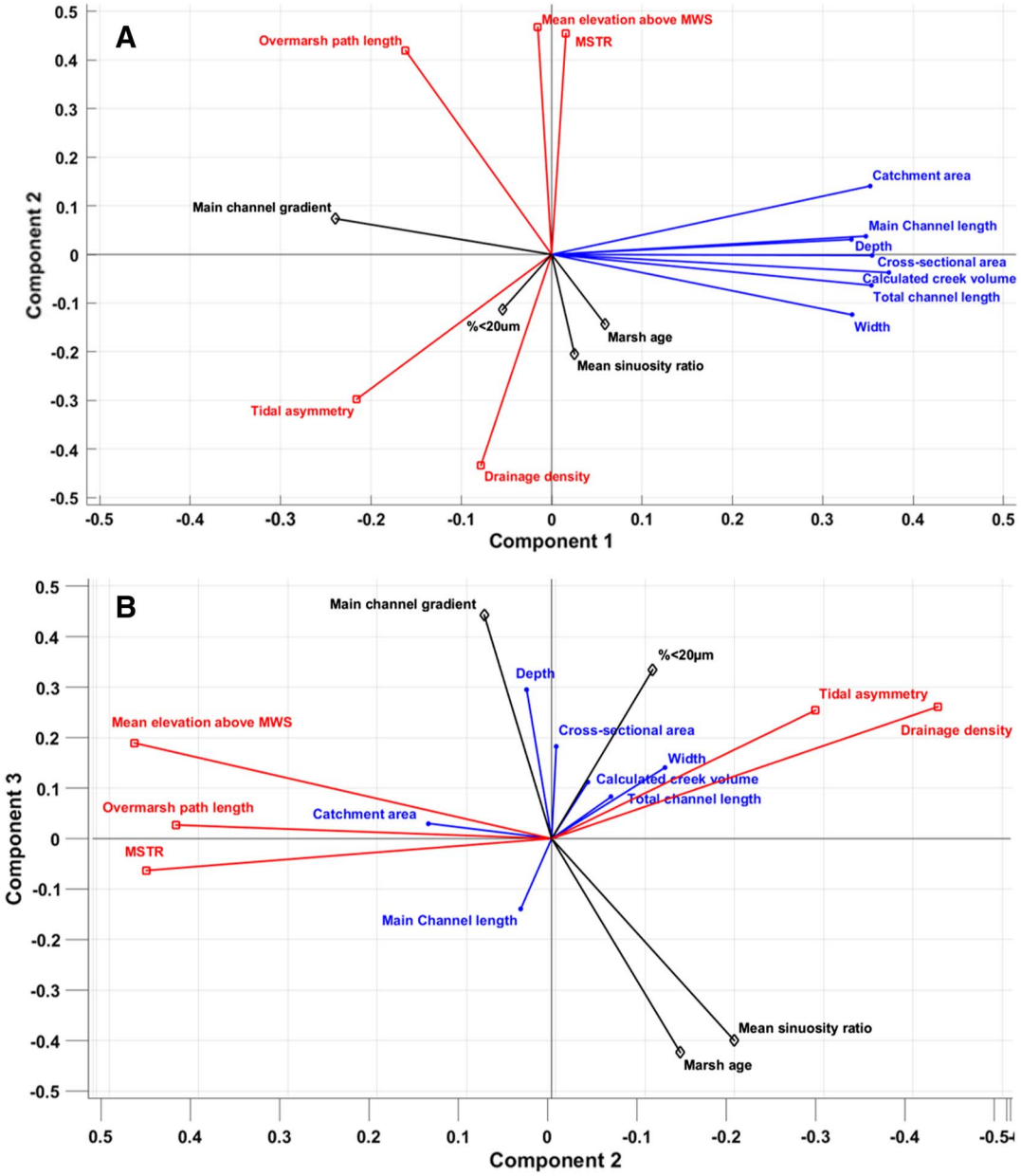

Fig. 15. Biplot of normalized variables for all sites except Crossens and Gibraltar Point, with the first three PCs as axes (Matlab function biplot). A: contributions of the variables to PC1 (blue dots) and PC2 (red squares). B: contributions of the variables to PC2 and PC3 (black diamonds). (For interpretation of the references to color in this figure legend, the reader is referred to the web version of this article.)

equilibrium relationships beyond the British saltmarshes considered here.

A more important limiting factor is the large number of variables influencing creek growth, which have not all been taken into consideration in this strictly morphological analysis. The variables considered here failed to explain the low OPL values at Gibraltar Point and Crossens. Other variables influencing creek network development include flow velocity (Zedler and Reed, 1995; Fagherazzi and Sun, 2004), wind waves (Callaghan et al., 2010), accretion rates within the marsh (Reed et al., 1999) and the sediment trapping and flow-rerouting action of the vegetation (Schwarz et al., 2014). Better knowledge of the hydrodynamic and sedimentological processes involved in MR creek network evolution should be obtained by coupling the lidar analysis with regular field surveys in at least one of the MR sites.

Another limit of this study concerns ground detection under a vegetation cover by lidar. Out of concern about altering the original lidar dataset as little as possible, and since the details of the EA vegetation removal algorithm are not publicly available, the raw lidar DSM have been used herein. This yielded good results for the creek network, as saltmarsh vegetation's height is typically not sufficient to impede creek detection (Mason and Scott, 2004). However, in MR schemes, plant colonization is expected within the span of a few years (Wolters et al., 2005), and could result in apparent elevation changes undiscernible from changes due to vertical accretion of sediment. Vegetation removal has been a major issue in previous lidar-based saltmarsh monitoring studies (Wang et al., 2009a): even state of the art lidar sensors fail to penetrate the saltmarsh canopy (Hladik and Alber, 2012). This limits the reliability of most DTMs in these environments. Correction algorithms have been developed by previous studies, based on vegetation cover detection by hyperspectral imagery, to approach the elevation of a bare saltmarsh (Hladik et al., 2013), but the DTM generated contained unrealistic “steps” which may interfere with creek detection.

Therefore, in order to verify the validity of elevation data in the developing saltmarshes of MR schemes, ground-truthing in the field is

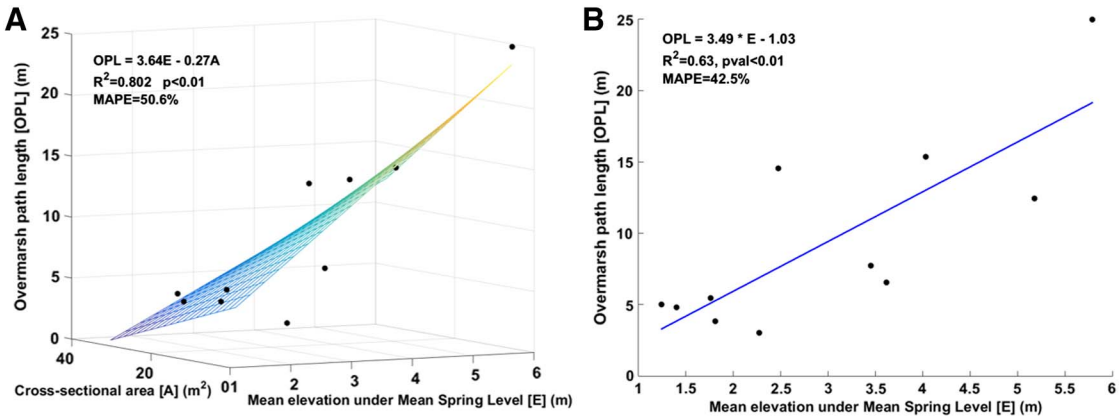

Fig. 16. A: Morphological relationship relating the overmarsh path length (OPL) to the mean marsh elevation relative to mean spring level (E) and to the cross-sectional area of the entry channel mouth or breach (A). Eq. [21] OPL = 3.64 E–0.27 A. B: Morphological relationship relating the overmarsh path length (OPL) to the mean marsh elevation relative to mean spring level (E). Eq. [22] OPL = 3.49 E–1.03.

necessary, especially along the creek network. RTK-GPS data can detect the bare ground at a vertical resolution of 1 to 4 cm (Montané and Torres, 2006). Ideally RTK-GPS surveying should be complemented by field measurements to assess the accretion/erosion rates in and around the creek network at a resolution of up to 1 mm (Kirby and Kirby, 2008). By coupling the accretion measurements with hydrodynamic data (water depth, flow velocity, suspended sediment concentration), monitoring and interpreting morphological changes occurring within MR schemes at multiple scales would become possible.

7. Conclusions

Our new semi-automated parametrization algorithm successfully extracted morphological characteristics of creek networks for 13 British saltmarshes. Despite the high variability of creek network shapes in natural saltmarshes, morphological relationships can be used to monitor trends of evolution towards equilibrium and determine which initial design choices encourage that evolution in managed realignment schemes. In addition to existing equilibrium relationships monitoring the channel length, depth and cross-sectional area, the overmarsh path length (OPL) is a valid proxy of the creek network's maturation stage. OPL represents the spatial distribution and drainage efficiency of the creek network, and is a relevant addition to the planimetric parameters already in use to determine morphological equilibrium. This paper is a first step towards providing design guidelines for creek networks, which will inform future design of managed realignment schemes and make their implementation as cost-effective as possible.

Acknowledgments

Funding for this project came from the University of Southampton (PhD stipend), with contributions from CH2M (CH2M/14664/01).

Appendix A. Supplementary data

Supplementary data to this article can be found online at https://doi.org/10.1016/j.rse.2017.11.012.

References

Admiralty Tide Tables, 2014. European Waters. vol. 1 H.M.S.O.
Ahn, C., Jones, S., 2013. Assessing organic matter and organic carbon contents in soils of created mitigation wetlands in Virginia. Environ. Eng. Res. 18 (3), 151–156. http://dx.doi.org/10.4491/eer.2013.18.3.151.
Allen, J.R.L., 2000. Morphodynamics of Holocene salt marshes: a review sketch from the Atlantic and Southern North Sea coasts of Europe. Quat. Sci. Rev. 19 (12), 1155–1231. http://dx.doi.org/10.1016/S0277-3791(99)00034-7.
Brzank, A., Heipke, C., Goepfert, J., Soergel, U., 2008. Aspects of generating precise digital terrain models in the Wadden Sea from lidar-water classification and structure line extraction. ISPRS J. Photogramm. Remote Sens. 63 (5), 510–528. http://dx.doi.org/10.1016/j.isprsjprs.2008.02.002.
Callaghan, D.P., Bouma, T.J., Klaassen, P., van der Wal, D., Stive, M.J.F., Herman, P.M.J., 2010. Hydrodynamic forcing on salt-marsh development: distinguishing the relative importance of waves and tidal flows. Estuar. Coast. Shelf Sci. 89 (1), 73–88. Elsevier Ltd. https://doi.org/10.1016/j.ecss.2010.05.013.
Chang, E.R., Veeneklaas, R.M., Bakker, J.P., Daniels, P., Esselink, P., 2016. What factors determined restoration success of a salt marsh ten years after de-embankment? Appl. Veg. Sci. 19 (1), 66–77. http://dx.doi.org/10.1111/avsc.12195.
Coco, G., Zhou, Z., Maanen, B., Van Olabarrieta, M., Tinoco, R., Townend, I., 2013. Morphodynamics of tidal networks: advances and challenges. Mar. Geol. 346, 1–16. Elsevier B.V. https://doi.org/10.1016/j.margeo.2013.08.005.
Committee on Climate Change, 2017. Progress in Preparing for Climate Change.
Crooks, S., Schutten, J., Sheern, G.D., Pye, K., Davy, A.J., 2002. Drainage and elevation as factors in the restoration of salt marsh in Britain. Restor. Ecol. 10 (3), 591–602. http://dx.doi.org/10.1046/j.1526-100X.2002.t01-1-0203.
D'Alpaos, A., Lanzoni, S., Marani, M., Fagherazzi, S., Rinaldo, A., 2005. Tidal network ontogeny: channel initiation and early development. J. Geophys. Res. Earth Surf. 110 (2), 1–14. http://dx.doi.org/10.1029/2004JF000182.
D'Alpaos, A., Lanzoni, S., Marani, M., Rinaldo, A., 2007. Landscape evolution in tidal embayments: modeling the interplay of erosion, sedimentation, and vegetation dynamics. J. Geophys. Res. Earth Surf. 112 (1), 1–17. http://dx.doi.org/10.1029/2006JF000537.
Davidson, N.C., 2014. How much wetland has the world lost? Long-term and recent trends in global wetland area. Mar. Freshw. Res. 65 (10), 934–941. http://dx.doi.org/10.1071/MF14173.
Doody, J.P., 2004. "Coastal squeeze" – an historical perspective. J. Coast. Conserv. 10 (1), 129–138. http://dx.doi.org/10.1652/1400-0350(2004)010[0129:CSAHP]2.0.CO;2.
Duarte, C.M., Dennison, W.C., Orth, R.J.W., Carruthers, T.J.B., 2008. The charisma of coastal ecosystems: addressing the imbalance. Estuar. Coasts 31 (2), 233–238. http://dx.doi.org/10.1007/s12237-008-9038-7.
Erwin, K.L., 2009. Wetlands and global climate change: the role of wetland restoration in a changing world. Wetl. Ecol. Manag. 17 (1), 71–84. http://dx.doi.org/10.1007/s11273-008-9119-1.
Esteves, L.S., 2014. Managed realignment: a viable long-term coastal management strategy? Springer Briefs in Environmental Science. Springer, New York, pp. 1–139. http://dx.doi.org/10.1007/978-94-017-9029-1.
Fagherazzi, S., Sun, T., 2004. A stochastic model for the formation of channel networks in tidal marshes. Geophys. Res. Lett. 31 (21), 1–4. http://dx.doi.org/10.1029/2004GL020965.
Fagherazzi, S., Bortoluzzi, A., Dietrich, W.E., Adami, A., Lanzoni, S., Marani, M., Rinaldo, A., 1999. Tidal networks 1. Automatic network extraction and preliminary scaling features from digital terrain maps. Water Resour. Res. 35 (12), 3891–3904. http://dx.doi.org/10.1029/1999WR900236.
Foster, N.M., Hudson, M.D., Bray, S., Nicholls, R.J., 2013. Intertidal mud fl at and salt-marsh conservation and sustainable use in the UK: a review. J. Environ. Manag. 126, 96–104. http://dx.doi.org/10.1016/j.jenvman.2013.04.015.
French, J., 2006. Tidal marsh sedimentation and resilience to environmental change: Exploratory modelling of tidal, sea-level and sediment supply forcing in predominantly allochthonous systems. Mar. Geol. 235 (1–4), 119–136. SPEC. ISS. https://doi.org/10.1016/j.margeo.2006.10.009.
French, J.R., Stoddart, D.R., 2001. Hydrodynamics of saltmarsh creek systems: implications for marsh morphological development and material exchange. Earth Surf. Process. Landf. 17, 235–252. http://dx.doi.org/10.1002/esp.329017030.
Friedrichs, C.T., Perry, J.E., 2001. Tidal salt marsh morphodynamics: a synthesis. J. Coast. Res. (Special Issue 27), 7–37. http://dx.doi.org/10.2307/25736162.
Gedan, K.B., Kirwan, M.L., Wolanski, E., Barbier, E.B., Silliman, B.R., 2011. The present and future role of coastal wetland vegetation in protecting shorelines: answering recent challenges to the paradigm. Clim. Chang. 7–29. http://dx.doi.org/10.1007/s10584-010-0003-7.

Hampshire, S.F., 2011. Evolution and Design of Tidal Creeks Within Managed Realignment Sites: a Study at Freiston Shore, Hampshire.
Hladik, C., Alber, M., 2012. Accuracy assessment and correction of a LIDAR-derived salt marsh digital elevation model. Remote Sens. Environ. 121, 224–235. Elsevier Inc.. https://doi.org/10.1016/j.rse.2012.01.018.
Hladik, C., Schalles, J., Alber, M., 2013. Remote Sensing of Environment Salt marsh elevation and habitat mapping using hyperspectral and LIDAR data. Remote Sens. Environ. 139, 318–330. Elsevier Inc.. https://doi.org/10.1016/j.rse.2013.08.003.
Hood, W.G., 2014. Differences in tidal channel network geometry between reference marshes and marshes restored by historical dike breaching. Ecol. Eng. 71, 563–573. Elsevier B.V.. https://doi.org/10.1016/j.ecoleng.2014.07.076.
Horton, R.E., 1945. Erosional development of streams and their drainage basins; hydrophysical approach to quantitative morphology. GSA Bull. 56 (3), 275–370. http://dx.doi.org/10.1130/0016-7606(1945)56[275:EDOSAT]2.0.CO;2.
Hughes, Z.J., 2012. Tidal channels on tidal flats and marshes. In: Davis, R.A., Dalrymple, R.W. (Eds.), Principles of Tidal Sedimentology. Springer Netherlands, Dordrecht, pp. 269–300. http://dx.doi.org/10.1007/978-94-007-0123-6.
J.B.l, H., Zedler, J.B., Boyer, K.E., Williams, G.D., Callaway, J.C., 1997. Influence of physical processes on the design, functioning and evolution of restored tidal wetlands in California (USA). Wetl. Ecol. Manag. 4 (2), 73–91. http://dx.doi.org/10.1007/BF01876230.
James, L., Hunt, K., 2010. The LiDAR-side of headwater streams mapping channel networks with high-resolution topographic data. Southeast. Geogr. 50 (4), 523–539. http://dx.doi.org/10.1353/sgo.2010.0009.
Jolliffe, I.T., 2002. Principal Component Analysis, Second Edition. Springer Series in Statistics 98. pp. 487. http://dx.doi.org/10.1007/b98835.
Kearney, W.S., Fagherazzi, S., 2016. Salt marsh vegetation promotes efficient tidal channel networks. In: Nature Communications. 7. Nature Publishing Group, pp. 12287. http://dx.doi.org/10.1038/ncomms12287.
Kirby, J.R., Kirby, R., 2008. Medium timescale stability of tidal mudflats in Bridgwater Bay, Bristol Channel, UK: influence of tides, waves and climate. Cont. Shelf Res. 28 (19), 2615–2629. http://dx.doi.org/10.1016/j.csr.2008.08.006.
Lang, M., Mcdonough, O., Mccarty, G., 2012. Enhanced Detection of Wetland-Stream Connectivity Using LiDAR. pp. 461–473. http://dx.doi.org/10.1007/s13157-012-0279-7.
Lashermes, B., Foufoula-georgiou, E., Dietrich, W.E., 2007. Channel network extraction from high resolution topography using wavelets. Geophys. Res. Lett. 34, 1–6. http://dx.doi.org/10.1029/2007GL031140.
Liu, X., 2008. Airborne LiDAR for DEM generation: some critical issues. Prog. Phys. Geogr. 32 (1), 31–49. http://dx.doi.org/10.1177/0309133308089496.
Liu, Y., Zhou, M., Zhao, S., Zhan, W., Yang, K., Li, M., 2015. Automated extraction of tidal creeks from airborne laser altimetry data. J. Hydrol. 527, 1006–1020. Elsevier B.V.. https://doi.org/10.1016/j.jhydrol.2015.05.058.
Lohani, B., Mason, D.C., 2001. Application of airborne scanning laser altimetry to the study of tidal channel geomorphology. ISPRS J. Photogramm. Remote Sens. 56 (2), 100–120. http://dx.doi.org/10.1016/S0924-2716(01)00041-7.
Lohani, B., Mason, D.C., Scott, T.R., Sreenivas, B., Mason, D.C., Scott, T.R., Extraction, B.S., 2006. Extraction of tidal channel networks from aerial photographs alone and combined with laser altimetry. Int. J. Remote Sens. 27 (1), 5–25. http://dx.doi.org/10.1080/01431160500206692.
Lotze, H.K., Lenihan, H.S., Bourque, B.J., Bradbury, R.H., Cooke, G., Kay, M.C., Kidwell, S.M., Kirby, M.X., Peterson, C.H., Jackson, J.B.C., 2006. Depletion, degredation, and recovery potential of estuaries and coastal seas. Science 312 (5781), 1806–1809. http://dx.doi.org/10.1126/science.1128035.
Luisetti, T., Turner, R.K., Jickells, T., Andrews, J., Elliott, M., Schaafsma, M., Beaumont, N., Malcolm, S., Burdon, D., Adams, C., Watts, W., 2014. Coastal Zone Ecosystem Services: From science to values and decision making; a case study. Sci. Total Environ. 493C, 682–693. Elsevier B.V.. https://doi.org/10.1016/j.scitotenv.2014.05.099.
Manson, S., Pinnington, N., 2012. Alkborough Managed Realignment Measure Analysis. 30.
Marani, M., Belluco, E., D'Alpaos, A., Defina, A., Lanzoni, S., Rinaldo, A., 2003. On the drainage density of tidal networks. Water Resour. Res. 39 (2), 1–11. http://dx.doi.org/10.1029/2001WR001051.
Mason, D.C., Scott, T.R., 2004. Remote sensing of tidal networks and their relation to vegetation. In: The Ecogeomorphology of Tidal Salt Marshes, pp. 27–46. http://dx.doi.org/10.1029/CE059p0027.
Mason, D.C., Scott, T.R., Wang, H., 2006. Extraction of tidal channel networks from airborne scanning laser altimetry. ISPRS J. Photogramm. Remote Sens. 61, 67–83. http://dx.doi.org/10.1016/j.isprsjprs.2006.08.003.
Mehta, A.J., Lee, S.C., 1994. Problems in linking the threshold condition for the transport of cohesionless and cohesive sediment grain. J. Coast. Res. 10 (1), 170–177.
Miller, J. a, Simenstad, C. a, 1997. A comparative assessment of a natural and created estuarine slough as rearing habitat for juvenile chinook and coho salmon. Estuaries 20 (4), 792. http://dx.doi.org/10.2307/1352252.
Möller, I., Spencer, T., 2002. Wave dissipation over macro-tidal saltmarshes: Effects of marsh edge typology and vegetation change. J. Coast. Res. (0749-0208) 36 (36), 506–521.
Montané, J.M., Torres, R., 2006. Accuracy Assessment of Lidar Saltmarsh Topographic Data Using RTK GPS. Photogramm. Eng. Remote Sens. 72, 961–967. August. 10.14358/PERS.72.8.961.
Mossman, H.L., Davy, A.J., Grant, A., 2012. Does managed coastal realignment create saltmarshes with "equivalent biological characteristics" to natural reference sites? C Elphick (ed.). J. Appl. Ecol. 49 (6), 1446–1456. http://dx.doi.org/10.1111/j.1365-2664.2012.02198.x.
Mudd, S.M., 2011. The life and death of salt marshes in response to anthropogenic disturbance of sediment supply. Geology 39 (5), 511–512. http://dx.doi.org/10.1016/j.
Novakowski, K.I., Torres, R., Gardner, R., Voulgaris, G., 2004. Geomorphic analysis of tidal creek networks. Water Resour. Res. 40 (5). http://dx.doi.org/10.1029/2003WR002722.
Ozdemir, H., Bird, D., 2009. Evaluation of morphometric parameters of drainage networks derived from topographic maps and DEM in point of floods. Environ. Geol. 56 (7), 1405–1415. http://dx.doi.org/10.1007/s00254-008-1235-y.
Passalacqua, P., Trung, T., Do Foufoula-georgiou, E., Sapiro, G., Dietrich, W.E., 2010. A geometric framework for channel network extraction from lidar: nonlinear diffusion and geodesic paths. J. Geophys. Res. 115, 1–18. http://dx.doi.org/10.1029/2009JF001254.
Pontee, N.I., 2003. Designing sustainable estuarine intertidal habitats. Eng. Sustain. 156 (ES3), 157–167. http://dx.doi.org/10.1680/ensu.2003.156.3.157.
Pontee, N., 2015. Hydromorphological considerations for the restorations of intertidal habitats. In: Coastal Sediments Conference 2015.
Rapinel, S., Clément, B., Nabucet, J., Cudennec, C., 2015. Ditch network extraction and hydrogeomorphological characterization using LiDAR-derived DTM in wetlands. Hydrol. Res. 46 (2), 276–290. http://dx.doi.org/10.2166/nh.2013.121.
Reed, D.J., Spencer, T., Murray, A.L., French, J.R., Leonard, L., 1999. Marsh surface sediment deposition and the role of tidal creeks: implications for created and managed coastal marshes. J. Coast. Conserv. 5, 81–90. http://dx.doi.org/10.1007/BF02802742.
Rogers, K., Saintilan, N., Copeland, C., 2014. Managed retreat of saline coastal wetlands: challenges and opportunities identified from the Hunter River estuary, Australia. Estuar. Coasts 37 (1), 67–78. http://dx.doi.org/10.1007/s12237-013-9664-6.
Rupp-Armstrong, S., Nicholls, R.J., 2007. Coastal and estuarine retreat: a comparison of the application of managed realignment in England and Germany. J. Coast. Conserv. 23 (6), 1418–1431. http://dx.doi.org/10.2112/04-0426.1.
Sanderson, E.W., Ustin, S.L., Foin, T.C., 2000. The influence of tidal channels on the distribution of salt marsh plant species in Petaluma Marsh, CA, USA. Plant Ecol. 146 (1), 29–41. http://dx.doi.org/10.1023/A:1009882110988.
Sanderson, E.W., Foin, T.C., Ustin, S.L., 2001. A simple empirical model of salt marsh plant spatial distributions with respect to a tidal channel network. Ecol. Model. 139 (2–3), 293–307. http://dx.doi.org/10.1016/S0304-3800(01)00253-8.
Schwarz, C., Ye, Q.H., van der Wal, D., Zhang, L.Q., Bouma, T., Ysebaert, T., Herman, P.M.J., 2014. Impacts of salt marsh plants on tidal channel initiation and inheritance. J. Geophys. Res. Earth Surf. 119, 385–400. http://dx.doi.org/10.1002/2013JF003034.Received.
Spencer, K.L., Harvey, G.L., 2012. Understanding system disturbance and ecosystem services in restored saltmarshes: integrating physical and biogeochemical processes. Estuar. Coast. Shelf Sci. 106, 23–32. Elsevier Ltd. https://doi.org/10.1016/j.ecss.2012.04.020.
Steel, T.J., 1996. The Morphology and Development of Representative British Saltmarsh Creek Networks.
Steel, T.J., Pye, K., 1997. The development of saltmarsh tidal creek networks: evidence from the UK. In: Canadian Coastal Conference, pp. 267–280.
Strahler, A.N., 1957. Quantitative analysis of watershed geomorphology. EOS Trans. Am. Geophys. Union 38 (6), 913–920. http://dx.doi.org/10.1029/TR038i006p00913.
Symonds, A.M., 2006. Impacts of Coastal Realignment on Intertidal Sediment Dynamics: Freiston Shore, The Wash.
Temmerman, S., Bouma, T.J., Govers, G., Wang, Z.B., De Vries, M.B., Herman, P.M.J., 2005. Impact of vegetation on flow routing and sedimentation patterns: three-dimensional modeling for a tidal marsh. J. Geophys. Res. Earth Surf. 110 (4), 1–18. http://dx.doi.org/10.1029/2005JF000301.
Tempest, J. a, Harvey, G.L., Spencer, K.L., 2014. Modified sediments and subsurface hydrology in natural and recreated salt marshes and implications for delivery of ecosystem services. Hydrol. Process. 29, 2346–2357. http://dx.doi.org/10.1002/hyp.10368.
Tovey, E.L., Pontee, N.I., Harvey, R., 2009. Managed realignment at Hesketh out marsh west. Eng. Sustain. 162 (ES4), 223–228. http://dx.doi.org/10.1680/ensu.2009.162.
Townend, I.H., 2008. Breach design for managed realignment sites. Proc. ICE Marit. Eng. 161 (1), 9–21. http://dx.doi.org/10.1680/maen.2008.161.1.9.
Uylings, H.B.M., Smit, G.J., Veltman, W. a, 1975. Ordering methods in quantitative analysis of branching structures of dendritic trees. Adv. Neurol. 12, 347–354.
Van Der Wal, D., Pye, K., Neal, A., 2002. Long-term morphological change in the Ribble Estuary, northwest England. Mar. Geol. 189 (3–4), 249–266. http://dx.doi.org/10.1016/S0025-3227(02)00476-0.
Vandenbruwaene, W., Meire, P., Temmerman, S., 2012. Formation and evolution of a tidal channel network within a constructed tidal marsh. Geomorphology 151–152, 114–125. Elsevier B.V.. https://doi.org/10.1016/j.geomorph.2012.01.022.
Vandenbruwaene, W., Bouma, T.J., Meire, P., Temmerman, S., 2013. Bio-geomorphic effects on tidal channel evolution: impact of vegetation establishment and tidal prism change. Earth Surf. Process. Landf. 38 (2), 122–132. http://dx.doi.org/10.1002/esp.3265.
Wallace, K.J., Callaway, J.C., Zedler, J.B., 2005. Evolution of tidal creek networks in a high sedimentation environment: a 5-year experiment at Tijuana Estuary, California. Estuaries 28 (6), 795–811. http://dx.doi.org/10.1007/BF02696010.
Wang, C., Menenti, M., Stoll, M.P., Feola, A., Belluco, E., Marani, M., 2009a. Separation of ground and low vegetation signatures in LiDAR measurements of salt-marsh environments. IEEE Trans. Geosci. Remote Sens. 47 (7), 2014–2023. http://dx.doi.org/10.1109/TGRS.2008.2010490.
Wang, W.C., Chau, K.W., Cheng, C.T., Qiu, L., 2009b. A comparison of performance of several artificial intelligence methods for forecasting monthly discharge time series. J. Hydrol. 374 (3–4), 294–306. Elsevier B.V.. https://doi.org/10.1016/j.jhydrol.2009.06.019.

Weishar, L.L., Teal, J.M., Hinkle, R., 2005. Stream order analysis in marsh restoration on Delaware Bay. Ecol. Eng. 25 (3), 252–259. http://dx.doi.org/10.1016/j.ecoleng.2005.04.003.

Williams, P., Faber, P., Madera, C., Valley, M., 2001. Salt marsh restoration experience in San Francisco Bay. J. Coast. Res. 27, 203–211.

Williams, P.B., Orr, M.K., Garrity, N.J., 2002. Hydraulic geometry: a geomorphic design tool for tidal marsh channel evolution in wetland restoration projects. Restor. Ecol. 10 (3), 577–590. http://dx.doi.org/10.1046/j.1526-100X.2002.t01-1-02035.x.

Wolters, M., Garbutt, A., Bakker, J.P., 2005. Salt-marsh restoration: evaluating the success of de-embankments in north-west Europe. Biol. Conserv. 123 (2), 249–268. http://dx.doi.org/10.1016/j.biocon.2004.11.013.

Zedler, J.B., Kercher, S., 2005. WETLAND RESOURCES: status, trends, ecosystem services, and restorability. Annu. Rev. Environ. Resour. 30 (1), 39–74. http://dx.doi.org/10.1146/annurev.energy.30.050504.144248.

Zedler, J.B., Reed, D., 1995. Design guidelines for tidal channels in coastal wetlands. Restor. Ecol. 10, 577–590 January 1995.

Zeff, M.L., 1999. Salt marsh tidal channel morphometry: applications for wetland creation and restoration. Restor. Ecol. 7 (2), 205–211. http://dx.doi.org/10.1046/j.1526-100X.1999.72013.x.

Zheng, Z., Zhou, Y., Tian, B., Ding, X., 2016. The spatial relationship between salt marsh vegetation patterns, soil elevation and tidal channels using remote sensing at Chongming Dongtan Nature Reserve, China. Acta Oceanol. Sin. 35 (4), 26–34. http://dx.doi.org/10.1007/s13131-016-0831-z.